3. Results

3.1 Bioinformatics analysis

Twelve multicopper oxidase genes were identified in the *Magnaporthe grisea* genome (www.broad.mit.edu). Eleven out of these were predicted to be extracellular using program Wolf PSORT (Horton *et al*., 2007). Sequences of known laccases from *Neurospora crassa* and *Cryphonectria parasitica*, along with all the multicopper oxidases from *M*. *grisea* were used to generate a phylogenetic tree using Neighbour-joining method. Phylogenetic trees were generated using the protein (**Figure 9**) sequences.

3.2 Expression profiling of multicopper oxidases of *M. grisea*

Starvation stress has been implicated to generate similar response as in pathogenicity of *M. grisea* in the host plants, especially nitrogen starvation (Talbot *et al*., 1997). Therefore relative expressions of 12 multicopper oxidases of *M. grisea* were checked in normal growth versus under nitrogen starvation. Fungus was grown in CM for 24h and RNA was extracted. Fungus was grown in CM for 48h to obtain initial biomass and then treared with nitrogen starvation for 24h. 1µg of total RNA was used to synthesise cDNA. qRT-PCR was carried out using 12 multicopper oxidases specific primers. The cDNA from nitrogen starved sample was used for qRT-PCR to monitor the fold induction of the 12 multicopper oxidases in nitrogen starvation. The calibrator used was *TUB* (*β-tubulin*), where the primers were designed to amplify 78 bp fragment.

Relative expression of MGG_08127.5 was highest in the normal growth (**Figure 10.A**). Most of the multicopper oxidases showed 2-4 fold induction under nitrogen starvation,

except MGG_02876.5, which showed ~15-fold induction, suggesting that this gene may have a role in fungal pathogenicity (**Figure 10.B**). MGG_08127.5 and MGG_02876.5 were selected for further analysis and were named as *MgLac*1 and *MgLac*2, respectively for our own convenience.

3.3 Align two sequence results

The two selected multicopper oxidases were further aligned using BLAST with the protein sequences of known laccases of *N. crassa* and *C. parasitica.* Alignment of the MGG_08127.5 with *N. crassa* and *C. parasitica* laccase showed 49% and 46% identity, respectively, at amino acid level and alignment of the MGG_02876.5 showed 32% and 34% identity respectively.

3.4 Heterologous expression and purification of *Mg*Lac1 and *Mg*Lac2

Both laccase genes were cloned into yeast expression vector 'pEG (KT)' so that they were translationally 'in frame' with Glutathione-S-Transferase (*GST*) gene. pEG(KT)*MgLac1* (**Figure 11.A)** and pEG(KT)*MgLac2* (**Figure 12.A)** were thus constructed. *S. cerevisiae* (s288C) was then transformed with vectors pEG(KT) *Mg*Lac1 **(Figure 11.B)** and pEG(KT)*Mg*Lac2 **(Figure 12.B)**. Four percent galactose was used to induce *GAL1* promoter driving the expression of GST*Mg*Lac1 and GST*Mg*Lac2. The expressed fusion protein from the yeast transformants was purified by affinity chromatography using GST purification module. The GST tag was removed from fusion proteins using thrombin protease. Both *Mg*Lac1 and *Mg*Lac2 resolved as a single
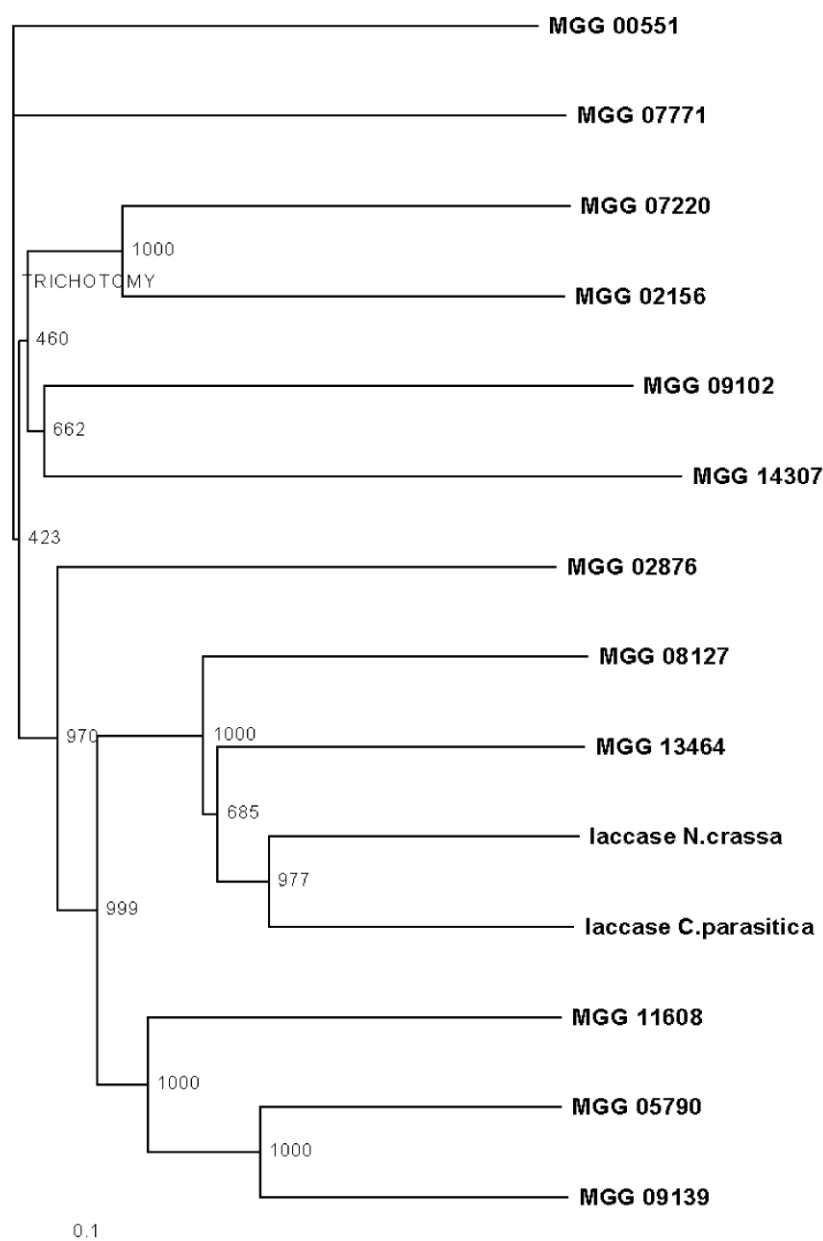
Figure 9: The phylogenetic analysis of 12 multicopper oxidase genes with other laccases from *N. crassa* and *C. parasitica*. Phylogenetic tree were generated by Neighbour-joining method based on the genetic distance of the protein sequences. Bootstrap values expressed as percentage (over 1000 replicates) are shown at the corresponding nodes.
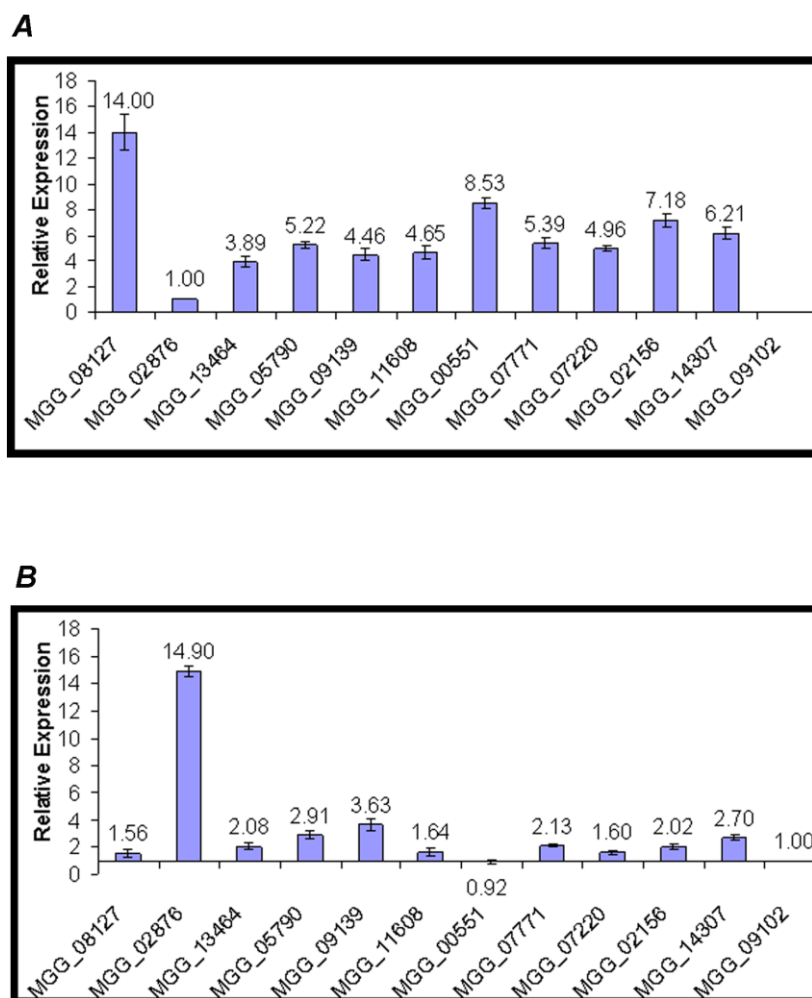
Figure 10: **(A)** Relative expression of 12 multicopper oxidases in *M. grisea*.

The relative expression level was compared with the lowest expressing multicopper oxidase. The values given are the average of triplicates. Bars indicate mean ± SD

(B) Response of the 12 multicopper oxidases to nitrogen starvation. *M. grisea* was grown in CM for 48 h and then in nitrogen starvation media for 24 h. The transcript levels were analysed by qRT-PCR. The relative induction levels were compared with the basal levels (taken as 1) observed in the normal condition. The values given are the average of triplicates. Bars indicate mean ± SD.
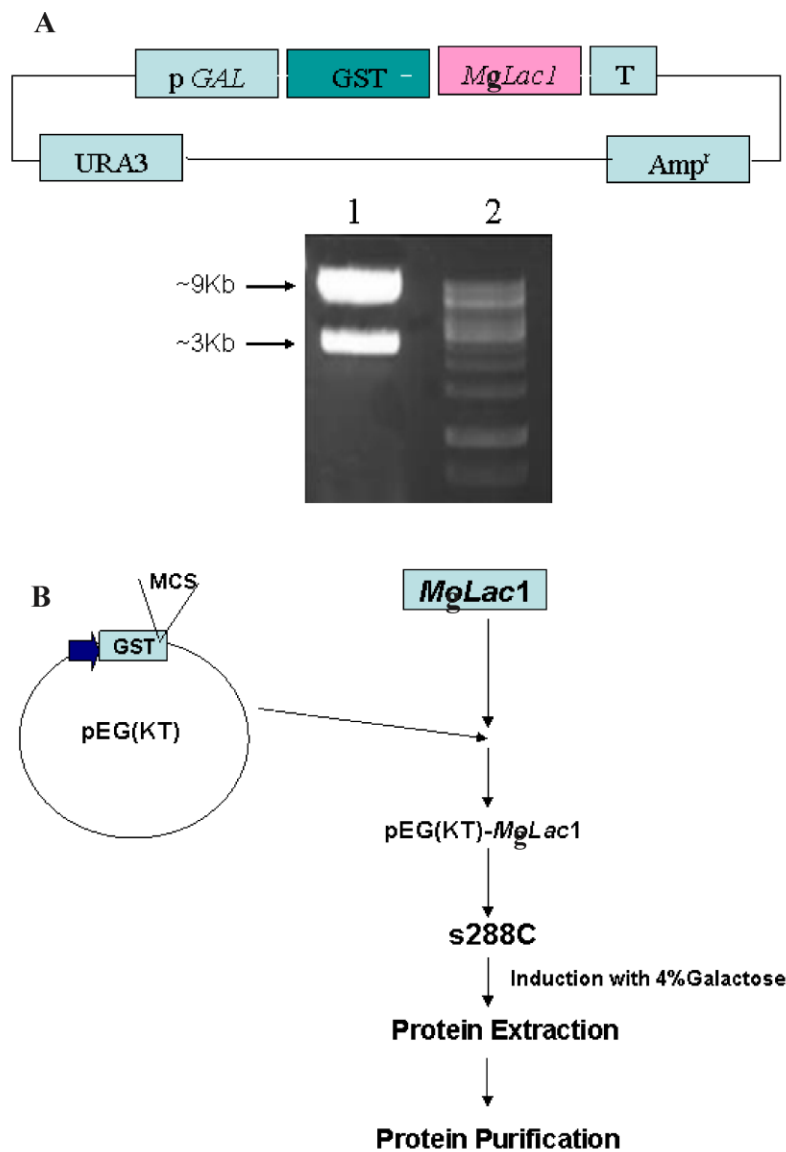
Figure 11: **(A)** Construction of heterologous expression vector pEG(KT)*MgLac1*. Confirmation of

pEG(KT)*MgLac1* by restriction digestion. Lane 1: pEG(KT)*MgLac1 Xho*I digestion, Lane 2: 1 Kb ladder.

(B) Steps involved in the expression and induction of *Mg*Lac1 in *S. cervisiae* s288C strain
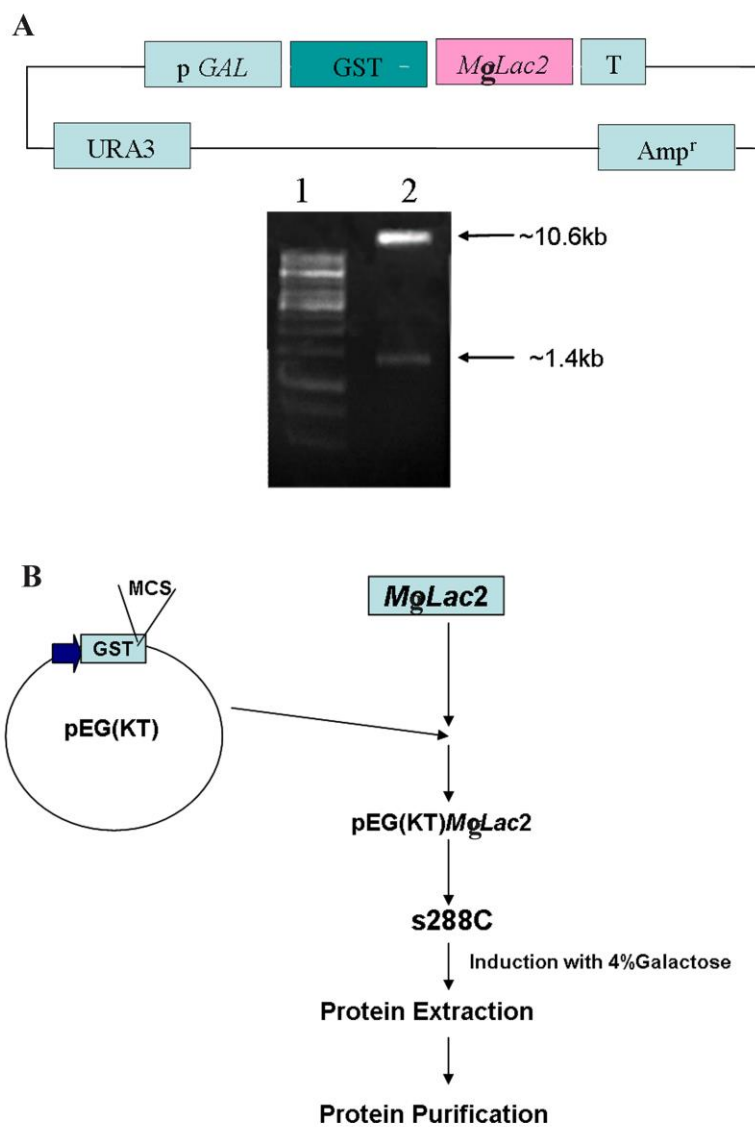
Figure 12: **(A)** Construction of heterologous expression vector pEG(KT)*MgLac*2. Confirmation of pEG(KT)*MgLac*2 by restriction digestion. Lane 1: 1 Kb ladder, Lane 2: pEG(KT)*MgLac*2 *Xho*I digestion. **(B)** Steps involved in the expression and induction of *Mg*Lac2 in *S. cervisiae* s288C strain

fragment of ~66 kDa on SDS–PAGE when stained with Coomassie Blue **(Figure 13)**. The purified *Mg*Lac1 and *Mg*Lac2 were subsequently used for studying the properties of these two enzymes.

3.5 Localisation of *Mg*Lac1 and *Mg*Lac2

*Mg*Lac1 and *Mg*Lac2 were predicted to be extracellular using program Wolf PSORT (Horton *et al*., 2007). These results were validated by western blot analysis using polyclonal antibodies raised against purified *Mg*Lac1 and *Mg*Lac2 in rabbit. ELISA was used to determine the titre of the antibodies and was found to be ~1600 for both. Our analysis revealed a clear band of ~66 kDa in culture filtrate of *M. grisea* which corresponds to the relative molecular weight (Mr) of *Mg*Lac1 and *Mg*Lac2. Such a band was not observed in case of intracellular proteins of *M. grisea,* confirming that the *Mg*Lac1 and *Mg*Lac2 both are secretory proteins **(Figure 14).**

3.6 Substrate specificity

The experimental kinetic data (averages of triplicate) was fitted mainly to single substrate (Michaelis-Menten) kinetics by nonlinear regression analysis. Kinetic parameters for the two laccases were evaluated for three substrates ABTS, Syringaldazine and DMP.

The Km values of *Mg*Lac1 and *Mg*Lac2 towards the various substrates indicated that the binding affinities towards different substrates were in the order: ABTS> Syringaldazine for both the enzymes and neither utilised DMP as substrate.
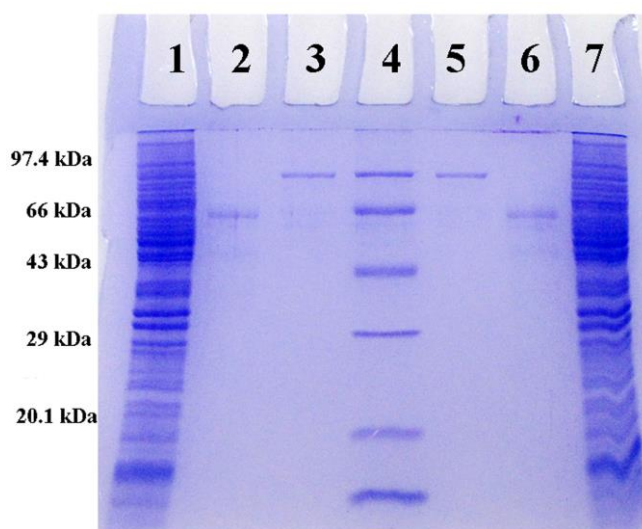
Figure 13: The protein purification. The fusion protein was purified by affinity chromatography using glutathione-sepharose as affinity matrix and the GST tag was removed from fusion proteins using thrombin protease. The purified proteins were checked on 12% SDS-PAGE.

Lane 1. Crude protein extract of s288C transformed with pEG(KT)*MgLac1* plasmid; Lane 2. Purified *Mg*Lac1; Lane 3. Purified GST-*Mg*Lac1; Lane 4. Molecular weight marker; Lane 5. Purified GST-*Mg*Lac2; Lane 6. Purified *Mg*Lac2; Lane 7. Crude protein extract of s288C transformed with pEG(KT)*MgLac2* plasmid.
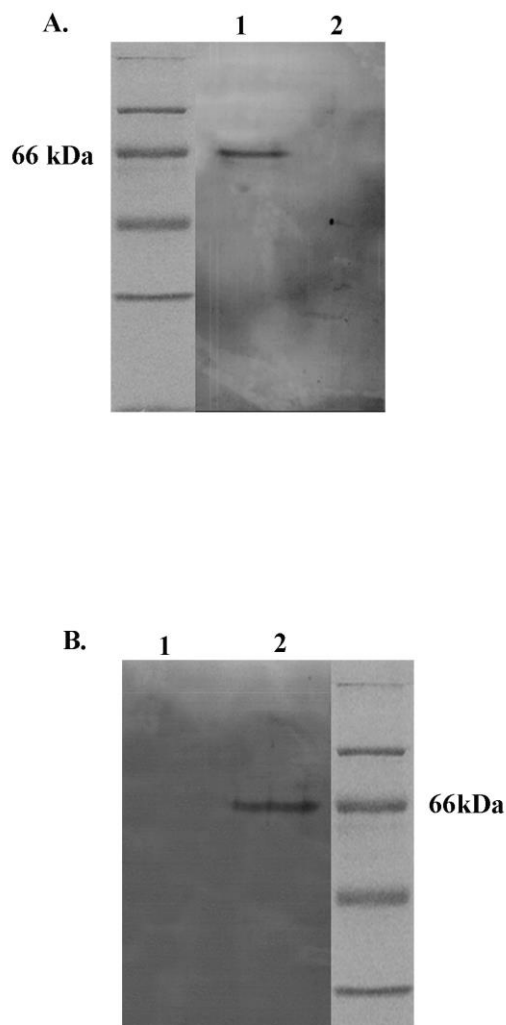
Figure 14: Western blot analysis. Polyclonal antibodies were raised in rabbit against *Mg*Lac1 and *Mg*Lac2, which were used for Western blot analysis.

(A) Western blot analysis of *Mg*Lac1 in intracellular proteins and culture filtrate of *M. grisea.* 1. Culture filtrate; 2. Intracellular proteins. 15 µg of protein was loaded in each well.

(B) Western blot analysis of *Mg*Lac2 in intracellular proteins and culture filtrate of *M. grisea.* 1. Intracellular proteins; 2. Culture filtrate. 15 µg of protein was loaded in each well.

Vm/Km ratios were expressed for the reactions of laccase towards the different substrates, as extinction coefficients are not available for all of the substrates studied. *Mg*Lac1 activity toward the substituted phenols was in the following order: meta>ortho>para substituted phenols. Catechol (-OH in ortho-position), as revealed by the Vm/Km ratios was more readily oxidised than its structural isomers Hydroquinone (-OH in para-position). No activity was noted for this para-substituted phenol whatsoever. *Mg*Lac1 could also oxidise Phloroglucinol. **(Figure 15; Table 4)**

*Mg*Lac2 activity toward the substituted phenols was in the following order: para>ortho>meta substituted phenols. Hydroquinone (-OH in para-position) as revealed by the Vm/Km ratios was more readily oxidised than its structural isomers Catechol (-OH in ortho-position). **(Figure 16; Table 4)**

3.7 Inhibition Studies

Laccase oxidises ABTS by abstraction of one electron to the stable, blue green radical cation (ABTS+). Laccase activity was inhibited by the addition of inhibitors and thus further formation of the radical cation was prevented. Experiments were performed in triplicate. *Mg*Lac1 was inhibited most efficiently by Sodium azide with lowest IC50.The inhibition was in the order; Sodium azide > Cysteine **>** EDTA > Chloride **(Figure 17; Table 5)**. *Mg*Lac2 was inhibited most efficiently by Cysteine with lowest IC50.The inhibition was in the order; Cysteine > Sodium azide > EDTA > Chloride **(Figure 18; Table 5)**.
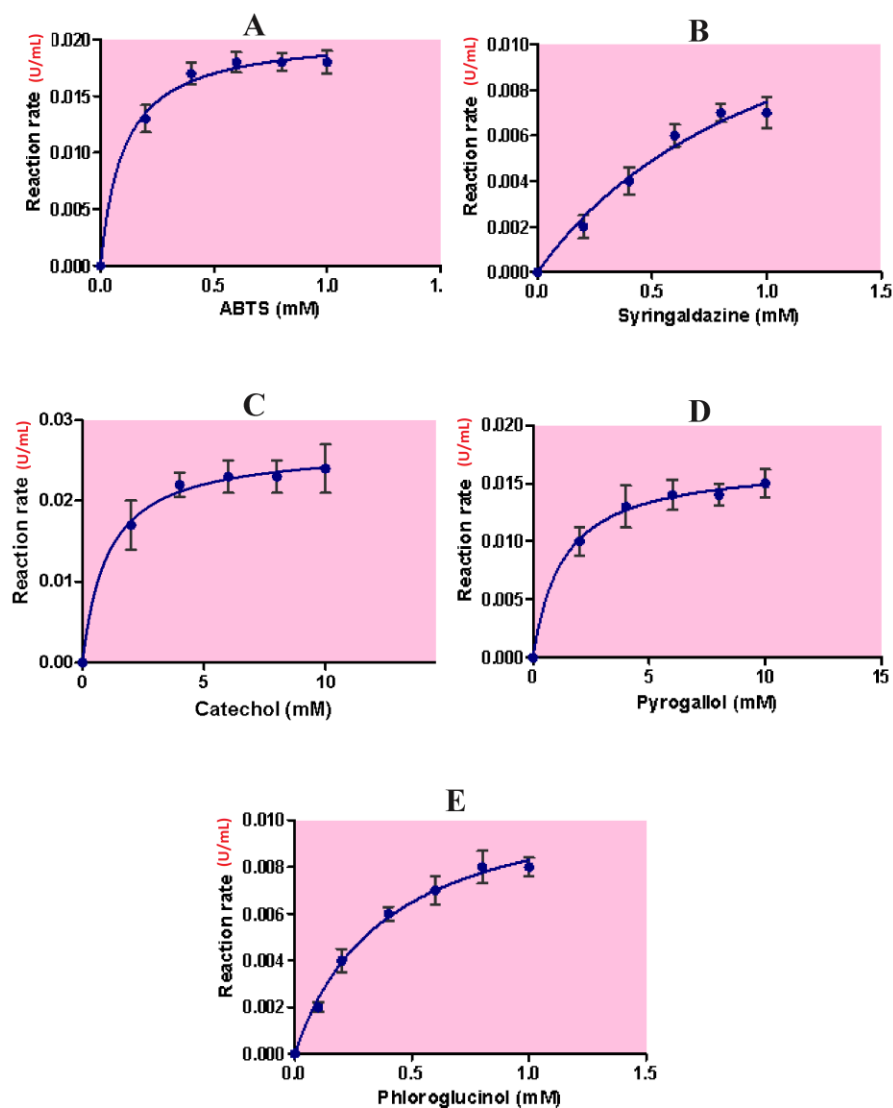
Figure 15: *In vitro* laccase activity of *Mg*Lac1. The purified *Mg*Lac1 was tested for laccase activity with different substrates. **A.** ABTS; **B.** Syringaldazine; **C.** Catechol**; D.** Pyrogallol; **E.** Phloroglucinol. The values given are the average of triplicates. Bars indicate mean ± SD.
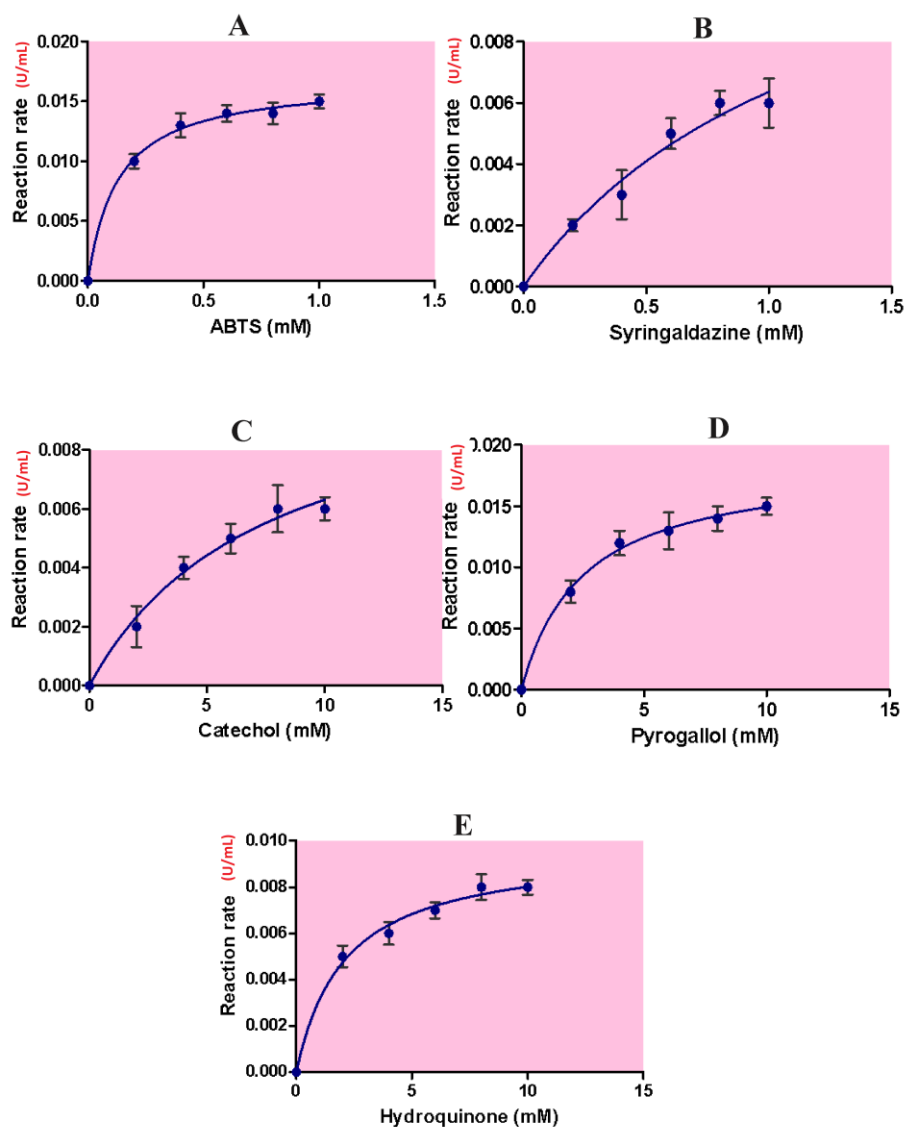
Figure 16: *In vitro* laccase activity of *Mg*Lac2. The purified *Mg*Lac2 was tested for laccase activity with different substrates. **A.** ABTS; **B.** Syringaldazine; **C.** Catechol**; D.** Pyrogallol; **E.** Hydroquinone. The values given are the average of triplicates. Bars indicate mean ± SD.

SUBSTRATE	*Mg* Lac1		*Mg* Lac2	
	Vmax	Km	Vmax	Km
ABTS	0.0205	0.1035	0.01681	0.1301
2,6-DMP	-	-	-	-
Syringaldazine	0.01579	1.113	0.01428	1.243
Guaiacol	-	-	-	-
Catechol	0.02666	1.047	0.011	7.432
Pyrogallol	0.01681	1.301	0.01866	2.509
Hydroquinone	-	-	0.00968	2.088
Phloroglucinol	0.01152	0.3894	-	-
Ferulic acid	-	-	-	-
Tyrosine	-	-	-	-

Table 4: Activity assays of *Mg*Lac1 and *Mg*Lac2 with ten different substrates. Experimental kinetic data (averages of triplicate data) was fitted to single substrate (Michaelis-Menten) kinetics by nonlinear regression analysis.
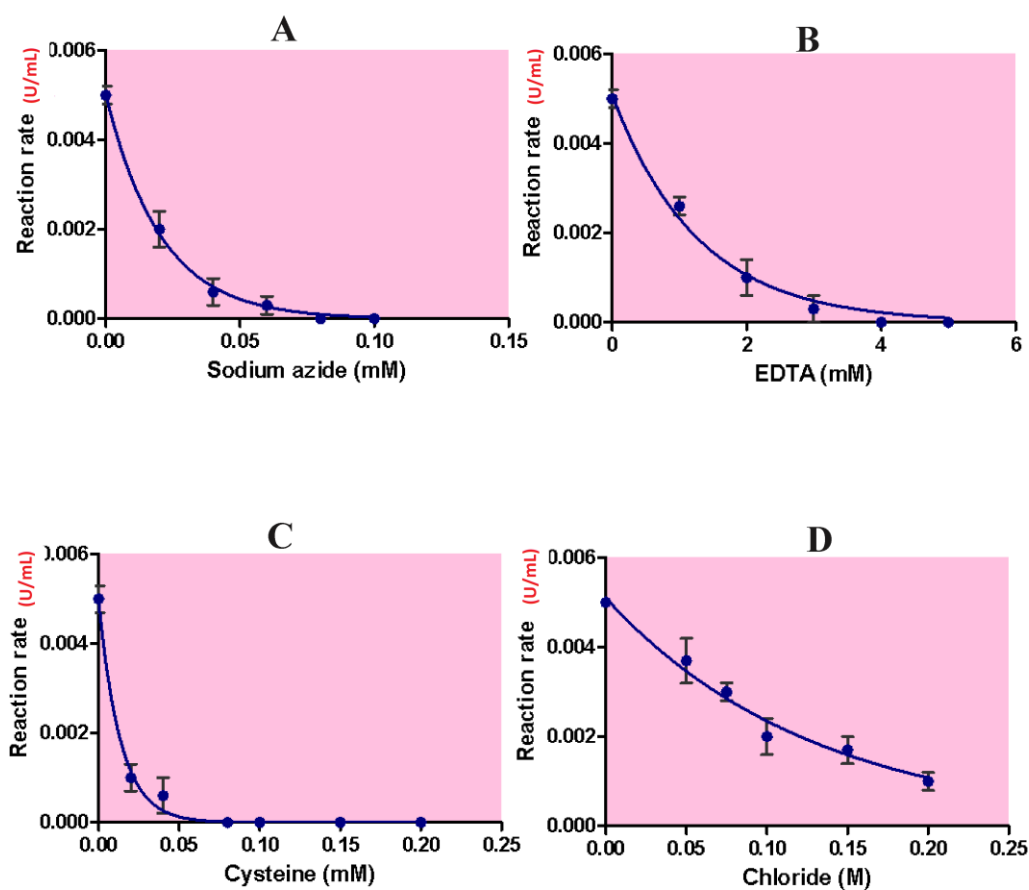
Figure 17: *In vitro* inhibition studies of *Mg*Lac1. The purified *Mg*Lac1 was tested with 4 different inhibitors. **A.** Sodium azide; **B.** EDTA; **C.** Cysteine**; D.** Chloride. The values given are the average of triplicates. Bars indicate mean ± SD.
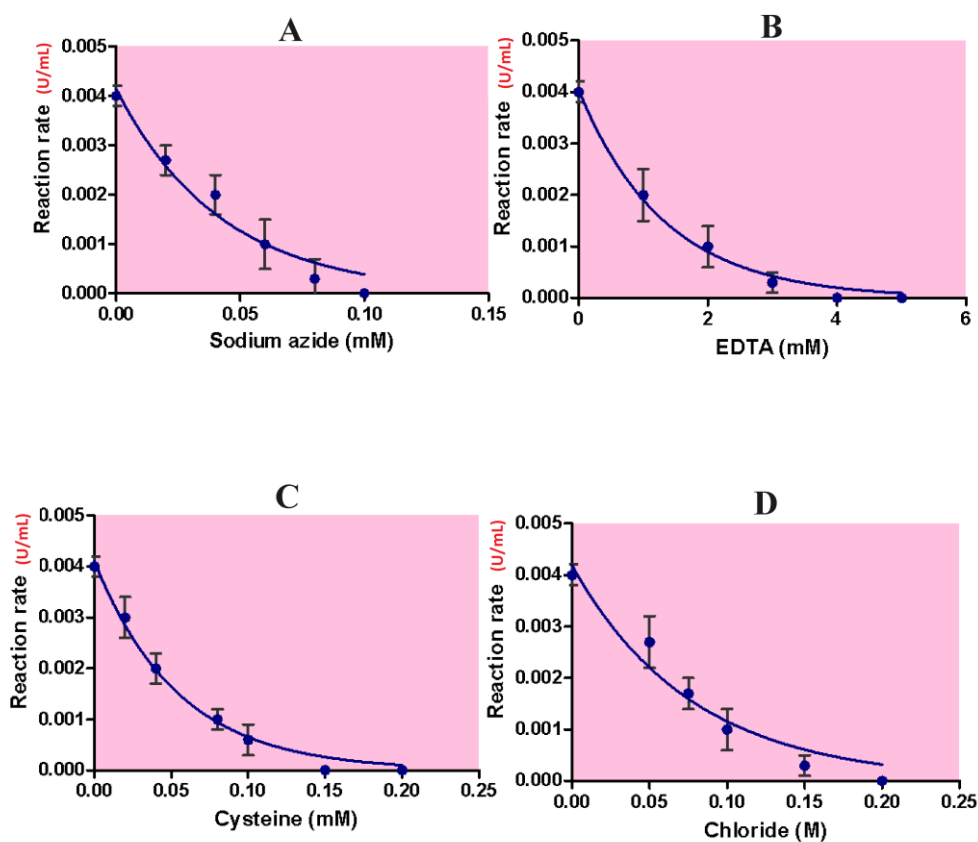
Figure 18: *In vitro* inhibition studies of *Mg*Lac2. The purified *Mg*Lac2 was tested with 4 different inhibitors. **A.** Sodium azide; **B.** EDTA; **C.** Cysteine**; D.** Chloride. The values given are the average of triplicates. Bars indicate mean ± SD.

SUBSTRATE	*Mg* Lac1 IC50 mM	*Mg* Lac2 IC50 mM
Sodium azide	0.6259	0.3744
EDTA	2.416	3.553
Cysteine	0.7321	0.2826
Chloride	53.31	164.3

Table 5: Inhibition studies of both the laccases. Experimental data was subjected to nonlinear regression analysis using the Dose-response-Inhibition equation and the kinetic parameter (IC50) was determined. Inhibition studies were performed with four different inhibitors. The values given are the average of triplicates.

3.8 Temperature effects and thermostability

Both proteins showed enzymatic activity over a remarkably wide range of temperatures. Significant enzyme activity was observed over the temperature range of 25^0C to 80^0C. Maximum thermostability of *Mg*Lac1 and *Mg*Lac2 was observed at 30^0C, when stored for 60 min **(Figure 19).**

3.9 Optimum pH

Three substrates were used to determine the effect of pH on laccase activity. The pH optima of the two laccases under study are in the range pH 3 to 5 which is typical for laccases (Luisa *et al.*, 1996). The pH optimum of *Mg*Lac1 is in between 4-5 **(Figure 20)** and that of *Mg*Lac2 is between 4-4.5 **(Figure 21)**.

3.10 Dye decolorisation activity

The purified *Mg*Lac1 and *Mg*Lac2 were used for determining decolourisation activity for Remazol brilliant blue dye. A fraction of empty vector transformed *S. cerevisiae* strain, s288C purified in an identical fashion was used as a negative control. Under our experimental conditions, *Mg*Lac1 and *Mg*Lac2 were able to decolourise Remazol Brilliant Blue dye **(Figure 22)**. Dye decolourisation assay was utilised to assess a possible role of these laccases in lignin degradation.
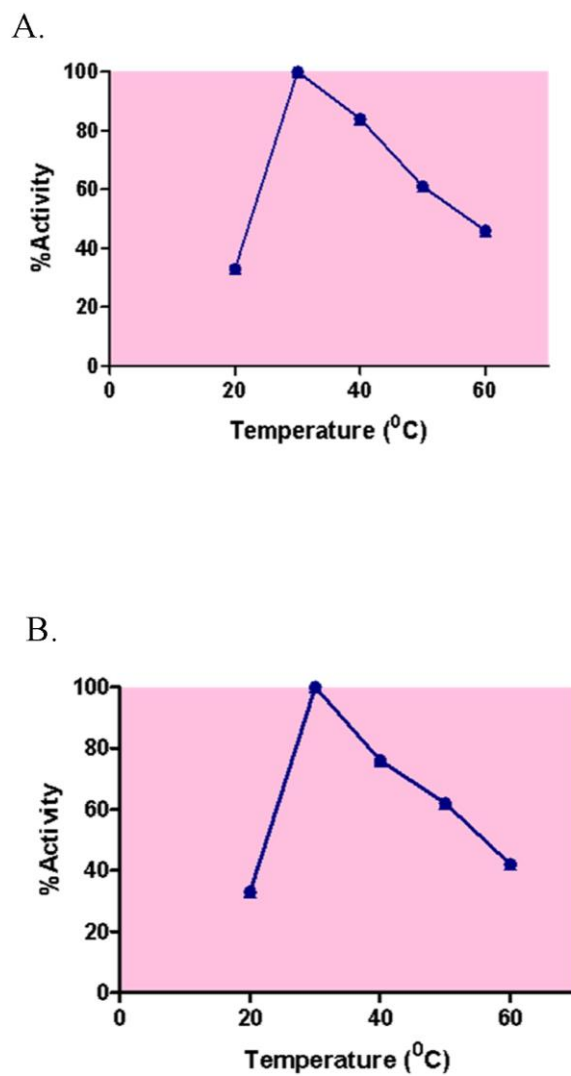
A.

B.

Figure 19: Thermostability studies of *Mg*Lac1 and *Mg*Lac2.

- **A.** The purified *Mg*Lac1 was tested for thermostability with ABTS at temperatures ranging from 20^0C to 60^0C at 10^0C intervals.

- **B.** The purified *Mg*Lac2 was tested for thermostability with ABTS at temperatures ranging from 20^0C to 60^0C at 10^0C intervals.
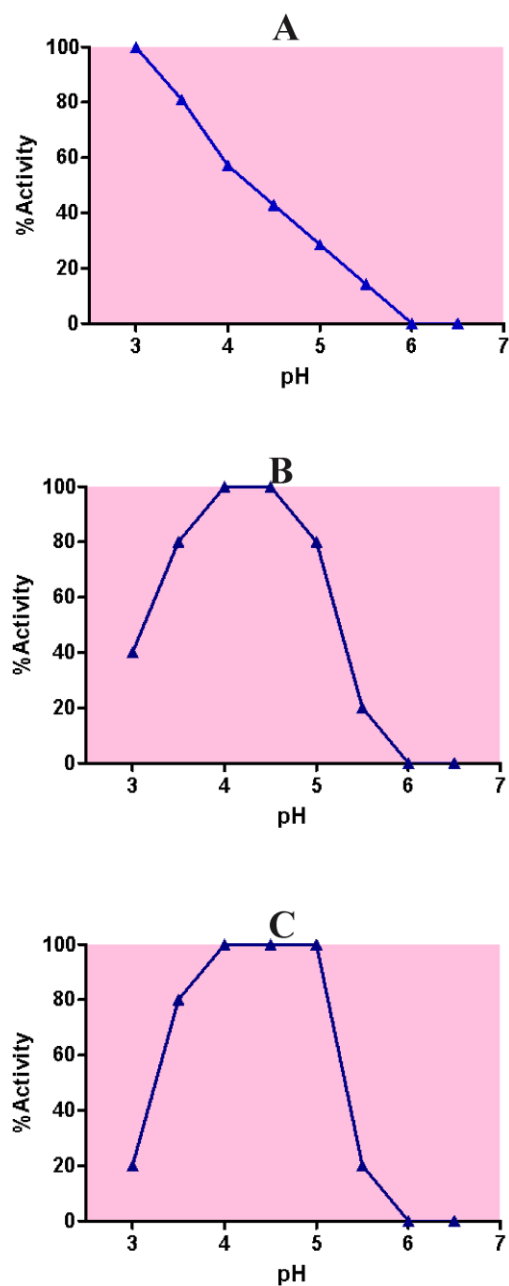
Figure 20: Optimum pH studies of *Mg*Lac1. The purified *Mg*Lac1 was tested with 3 different substrates.

A. ABTS; **B.** Catechol**; C.** Pyrogallol. The values given are the average of triplicates.
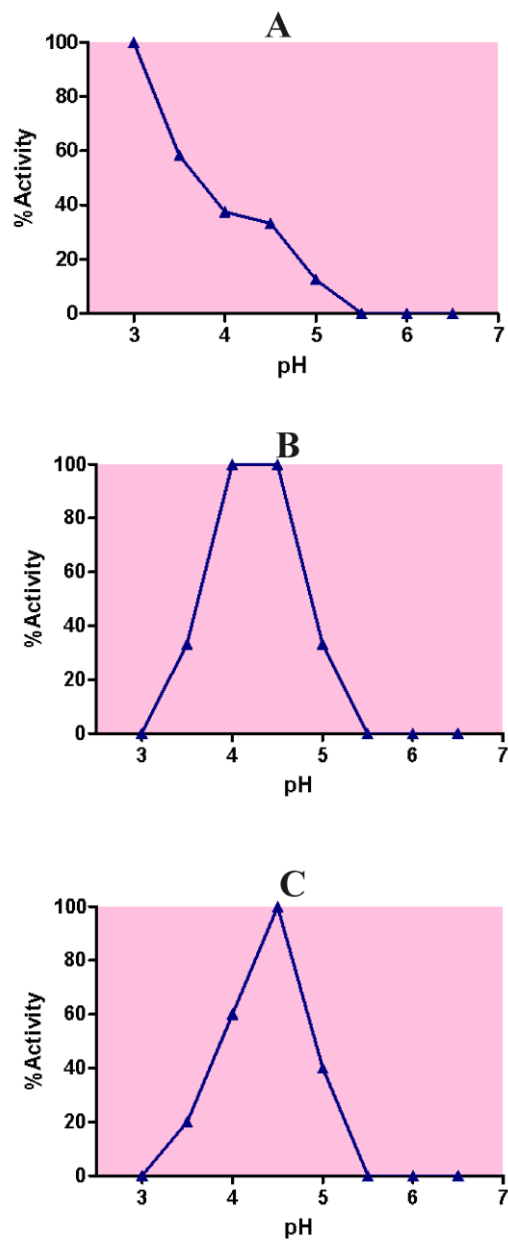
Figure 21: Optimum pH studies of *Mg*Lac2. The purified *Mg*Lac2 was tested with 3 different substrates.

A. ABTS; **B.** Catechol**; C.** Pyrogallol. The values given are the average of triplicates.
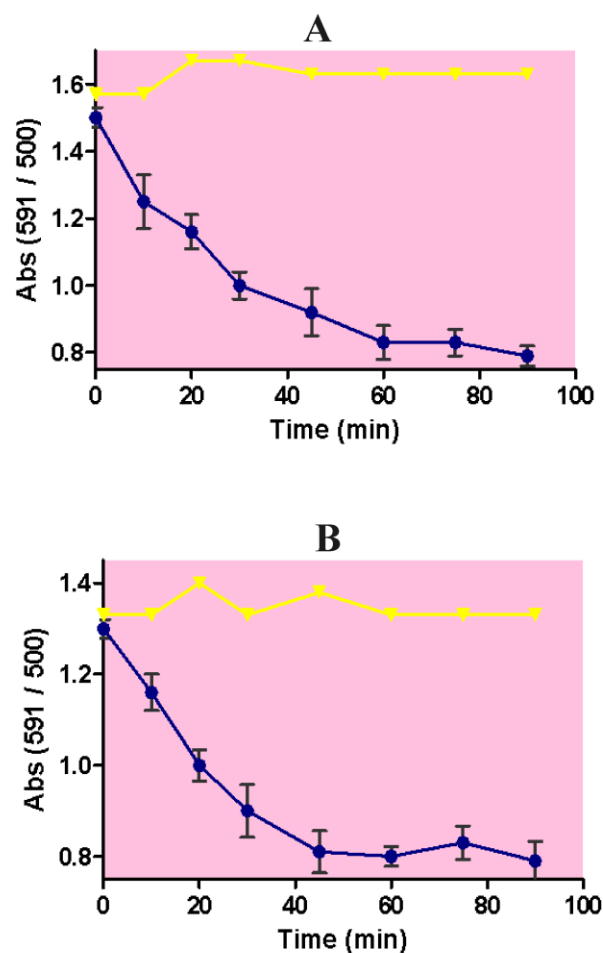
Figure 22: Dye decolorising activity was determined using Remazole brilliant blue R. Laccase (400 U) was added, and decolorisation was monitored spectrophotometrically after 0, 10, 20, 30, 45, 60, 75 and 90 min at 23^0C.

A. *Mg*Lac1: Decolorisation was observed when compared to control (without laccase). Control, (▼); *Mg*Lac1, (●).

B. *Mg*Lac2: Decolorisation was observed when compared to control (without laccase). Control, (▼); *Mg*Lac2, (●).

3.11 DHN polymerisation potential and Ferroxidase activity

*Mg*Lac2 polymerised DHN into a higher molecular mass melanin with maximum abosorbance at 348nm with an increase of 0.1 optical density units in 120 min (**Figure 23**). Ferroxidase activity was also detected in *Mg*Lac2 in addition to the above properties. The specific ferroxidase activity was 1.574×10^{-6} U/mg protein. *Mg*Lac1 did not show any DHN polymerisation potential and ferroxidase activity

3.12 Development of *MgLac*1 and *MgLac*2 antisense vector constructs

The coding region of *MgLac*1 (2198 bp) was amplified from genomic DNA of *M. grisea* using the specific primers The PCR amplified product was gel purified and restriction digested with *Xho*I and *Hind*III and cloned under *Trp*C promoter in antisense orientation in pSILENT vector to obtain plasmid pSILENT*MgLac*1. The desired cassette from pSILENT*MgLac*1 was then digested and cloned at *Xba*I site in binary vector pCAMBIA-1305.2 to obtain *MgLac*1 antisense vector **(Figure 24).**

The 1944bp coding region of *MgLac*2 was amplified from genomic DNA of *M. grisea* using the specific primers. The PCR amplified product was gel purified and restriction digested with *Bgl*II and *Kpn*I and cloned under *Trp*C promoter in antisense orientation in pSILENT vector to obtain plasmid pSILENT*MgLac2*. The desired cassette from pSILENT*MgLac2* was then digested and cloned at *Xba*I site in binary vector pCAMBIA-1305.2 to obtain *MgLac2* antisense vector **(Figure 25).**
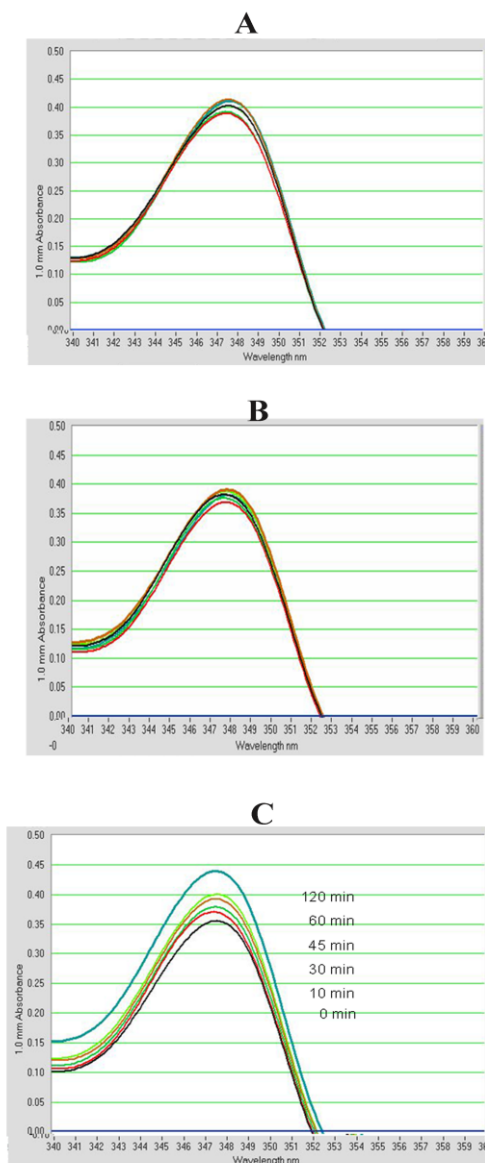
Figure 23: DHN polymerisation was estimated using Chromotropic acid disodium salts dehydrate. Laccase (15 U) was added, and polymerisation was monitored spectrophotometrically by scanning the solution from 320 to 520 nm at 0 to 120 min.

A. Control (without laccase): No change in absorbance was observed over the time period.

B. *Mg*Lac1: No change in absorbance was observed over the time period.

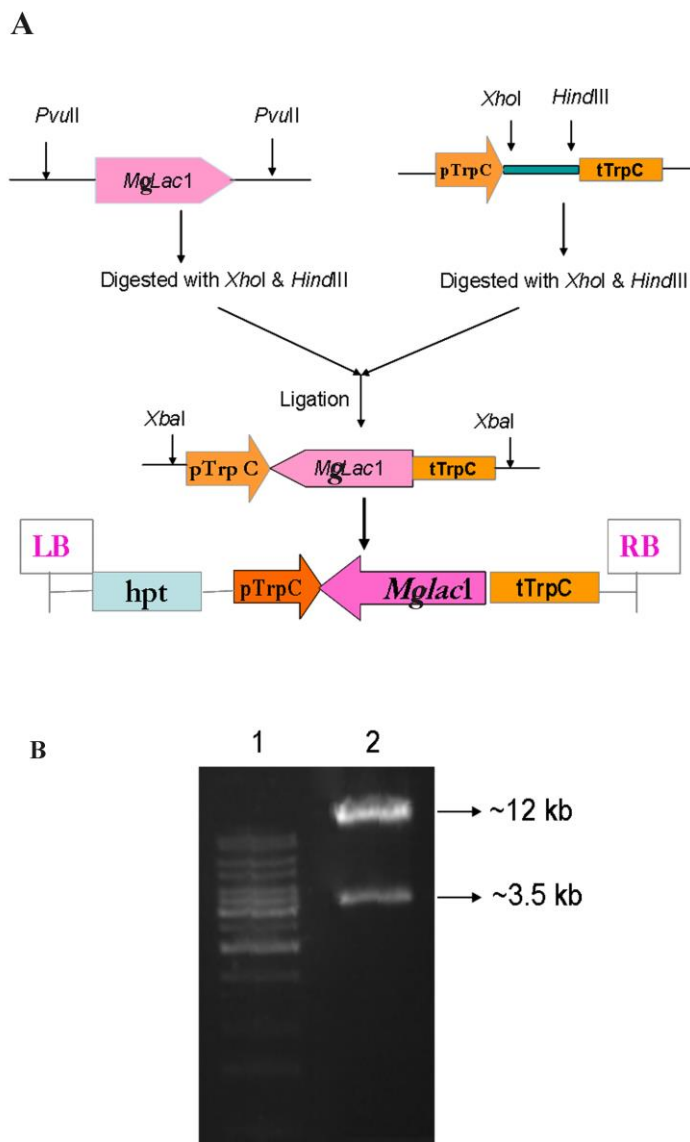**C.** *Mg*Lac2: Increase in absorbance was observed over the time period.

Figure 24: Construction of *MgLac*1 antisense vector

(A) The 2198 bp coding region of *MgLac*1 was amplified and the PCR product was digested with *Xho*I and *Hind*III and cloned into pSILENT vector digested with the same enzymes, to obtain pSILENT*MgLac*1. Plasmid pSILENT*MgLac*1 was then digested and cloned at *Xba*I site in pCAMBIA-1305.2.

(B) Confirmation of *MgLac1* antisense vector by restriction digestion with *Xba*I. Lane 1- 1 Kb ladder; Lane 2- *Xba*I digest.
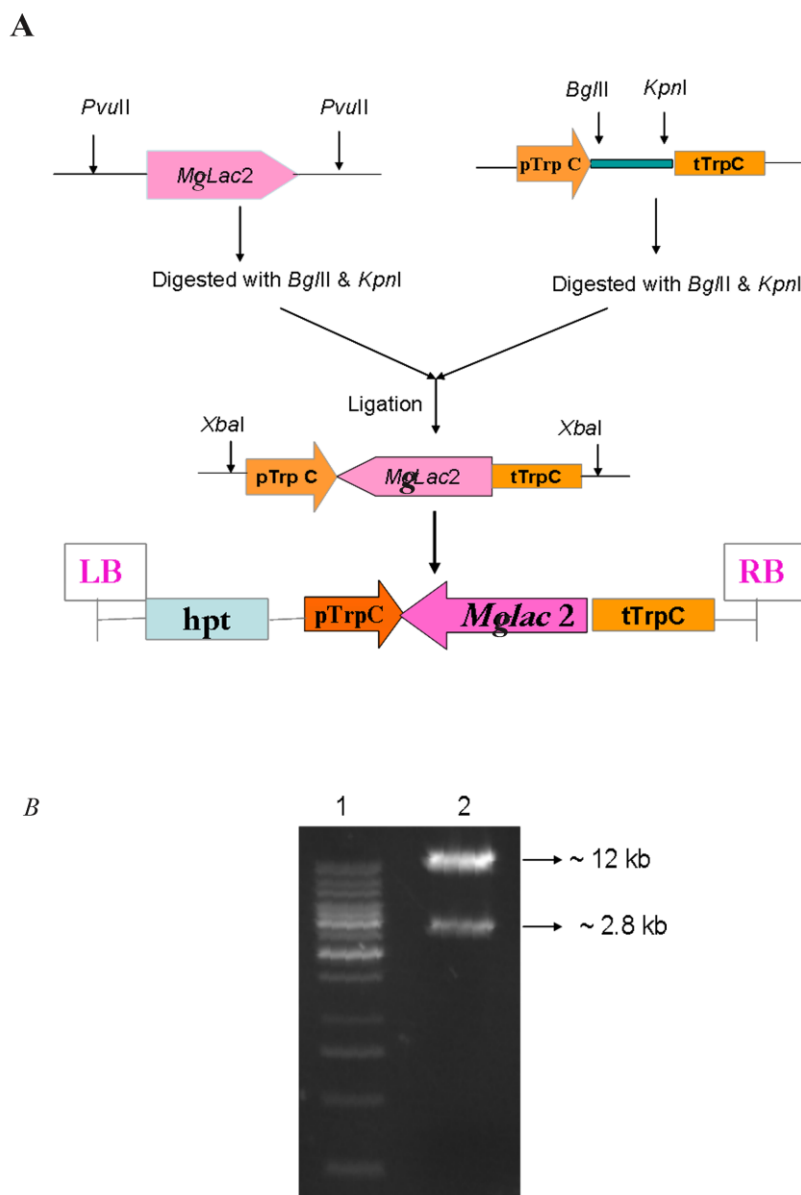
A

B

Figure 25: Construction of *MgLac2* antisense vector

(A) The 1944 bp coding region of *MgLac*2 was amplified and the PCR product was digested with *Bgl*II and *Kpn*I and cloned into pSILENT to obtain pSILENT*MgLac*2. Plasmid pSILENT*MgLac*2 was then digested and cloned at *Xba*I site in pCAMBIA-1305.2.

(B) Confirmation of *MgLac*2 antisense vector by restriction digestion with *Xba*I. Lane 1- 1 Kb ladder; Lane 2- *Xba*I digest

The antisense constructs of *MgLac1* and *MgLac2* were transferred into *Agrobacterium tumefaciens* strains LBA4404 by triparental mating. *A. tumefaciens* strain LBA4404 harbouring *MgLac1* and *MgLac2* antisense contructs were used for *M. grisea* transformation.

3.13 Agrobacterium tumefaciens mediated transformation of *M. grisea*

Knock-down transformants of *MgLac1* and *MgLac2* were obtained by *Agrobacterium tumefaciens* mediated transformation carried out in *M. grisea*. Transformants were selected on media containing Hygromycin B (200µg/ml). The transformation efficiency obtained was ~ 0.02% (200 transformants per 10^6 spores) **(Figure 26).**

3.14 Southern blot analysis

Integration patterns of the knockdown were studied by Southern blot analysis. Southern blot analysis was performed using genomic DNA from wild type fungus and *MgLac1* and *MgLac2* knock-down transformants. Genomic DNA from wild type fungus and transformants were digested with *Hind*III (cuts once in MCS of the T-DNA) and *Nde*I (cuts once in coding region of *hpt* gene) separately and then blotted onto nylon membrane. The coding region of *hpt* was used as a probe. Single insertion with different sites of integration was observed in both *MgLac1* **(Figure 27.A)** and *MgLac2* **(Figure 28.B)** knock-down transformants. However, no hybridisation was observed with the DNA of the wild type fungus**.**
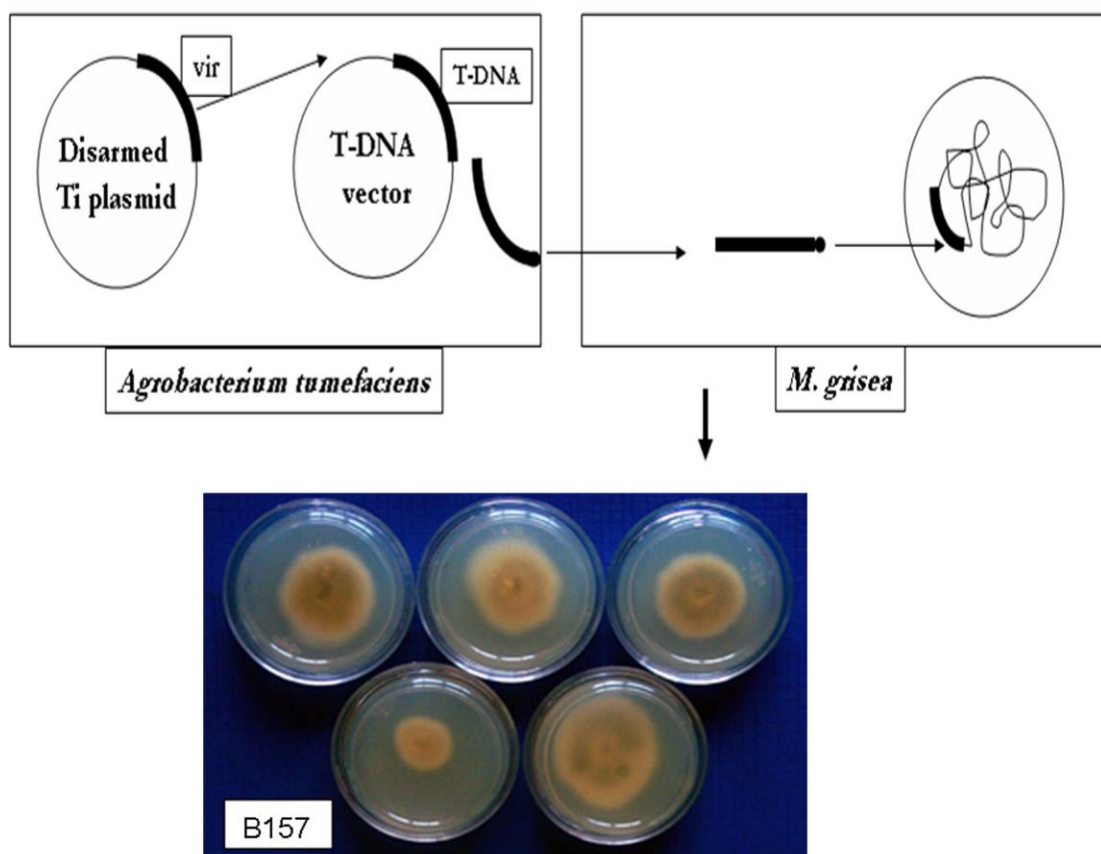
Figure 26: *Agrobacterium tumefaciens* mediated transformation of *M. grisea* (ATMT).

E. coli with donor plasmid (harbouring gene of interest within T-DNA), E. coli with helper plasmid, and *A. tumefaciens* with recipient plasmid are co-incubated during triparental mating for transfer of donor plasmid from *E. coli* to *Agrobacterium*. Fungal transformation results in transfer of the vector construct from *Agrobacterium* to *M. grisea* where T-DNA gets integrated into its genome. *M. grisea* was grown on YEG agar supplemented with 200 μg/ml Hygromycin B. Growth was observed after 5 days. Transformants showed growth on Hygromycin B whereas the wild type (B157) did not grow.
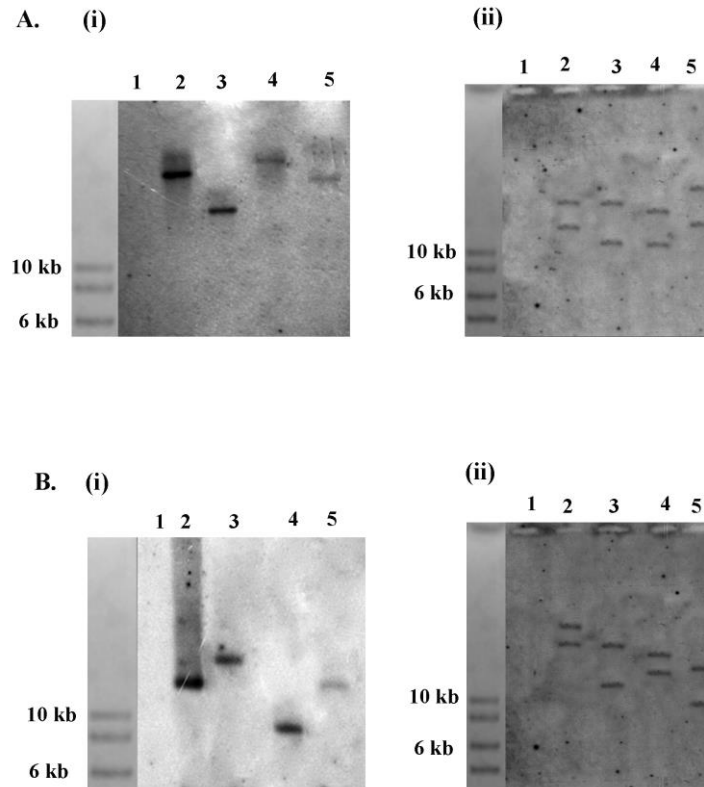
Figure 27: Southern blot analysis of *MgLac*1 and *MgLac*2 knock-down transformants. Genomic DNA (5 µg) was digested with restriction enzyme and blotted onto nitrocellulose membranes after electrophoresis in a 0.8% agarose gel. The membrane was hybridised with non-radioactively labelled coding region of *hpt*.

(A) Southern blot analysis of *MgLac*1 knock-down transformants where genomic DNA (5 µg) was digested with (i) *Hind*III (cuts once in MCS of the T-DNA). Lane 1: wild type B157; lane 2-6: *MgLac*1 knock-down transformants. (ii) *Nde*I (cuts once in coding region of *hpt* gene). Lane 1: wild type B157; lane 2-5: *MgLac*1 knock-down transformants.

(B) Southern blot analysis of *MgLac*2 knock-down transformants where genomic DNA (5 µg) was digested with (i) *Hind*III (cuts once in MCS of the T-DNA). Lane 1: wild type B157; lane 2-6: *MgLac*2 knock-down transformants. (ii) *Nde*I (cuts once in coding region of *hpt* gene). Lane 1: wild type B157; lane 2-5: *MgLac*1 knock-down transformants.

3.15 Expression of *MgLac*1 *and MgLac*2 in knock-down transformants

The knock-down transformants were analysed for expression of *MgLac*1 and *MgLac*2 at the mRNA level. *MgLac*1 and *MgLac*2 transcript levels were assayed by qRT-PCR in *MgLac*1 and *MgLac*2 knock-down transformants. Upto 88% of reduction in the transcript levels of *MgLac*1 (*MgLac*1.1 with 69%, *MgLac*1.2 with 88%, *MgLac*1.3 with 52% and *MgLac*1.4 with 35% knock-down) **(Figure 28.A)** and *MgLac2* (*MgLac*2.1 with 88%, *MgLac*2.2 with 67%, *MgLac*2.3 with 67% and *MgLac*2.4 with 66% knock-down) **(Figure 28.B)** in the respective knock-down transformants was obtained.

3.16 Phenotypic characterisation of *MgLac*1 knock-down transformants

Phenotypic characterisations of the *MgLac1* knock-down transformants were carried out. Growth, conidiation and appressorium formation **(Figure 29.A)** in the transformants were found to be comparable to the wild type. The wild type strain as well as knock-down transformants developed disease lesions on barley **(Figure 29.B)**. These results show that *MgLac1* is not involved in pathogenicity.

3.17 *MgLac*1 knock-down transformants grow better in presence of metals

Metal restricted growth assays were carried out in the presence EDTA (200μM) *MgLac*1 knock-down transformants showed less growth in presence of EDTA. The transformants showed growth upto ~79% of the normal growth of wild type B157 **(Figure 30.A).** The knock-down transformants showed more growth in presence of iron **(Figure 30.B)** copper **(Figure 30.C)** and NaCl **(Figure 30.D)** when compared to wild type. The growth of the transformants was ~116%, ~120% and 117% of wild type in presence of iron, copper and NaCl, respectively. But they became sensitive to $CaCl_2$ **(Figure 30.E)** and showed only 65 % of the wild type's growth.

As the knock-down transformants showed differential growth, elemental analysis of wild type *M. grisea* and knock-down transformants was done using X-ray fluorescence spectroscopy. Considerable differences were observed in the sulphur and phosphorus content of the transformants. The zinc, sulphur and phosphorus content of the transformants were ~119%, ~ 145% and ~ 201%, respectively, compared to the wild type B157. Potassium and iron content of the transformants were ~88% and ~92% compared to the wild type B157 (**Figure 31**).

3.18 Profile of laccase activity in B157 and *MgLac*1 knock-down transformants

Wild type B157 and the *MgLac*1.2 (88%) knock-down transformant were grown in liquid culture and the laccase activity was checked at different time points. In the wild type laccase activity was detected from 24 hours till 96 hours. In *MgLac*1.2 knock- down transformants the laccase activity after 24 hours was around 60% of the wild type (initial lag in laccase activity) which doubled after 48 hours and then came down to almost same activity after 96 hours (**Figure 32**).

3.19 Phenotypic characterisation of *MgLac*2 knock-down transformants

Phenotypic characterisations of the knock-down transformants were carried out and growth, melanin formation, conidiation and appressorium formation in the transformants were found to be comparable to the wild type. Interestingly, the knock-down transformants showed reduced aerial hyphae **(Figure 33.A)** compared to the wild type and underwent progressive
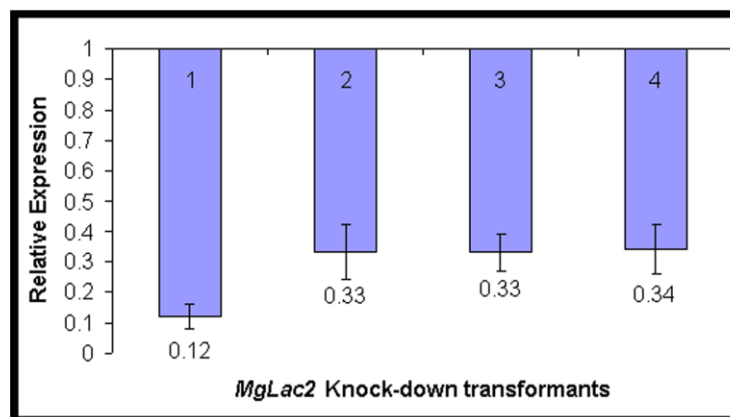
A.
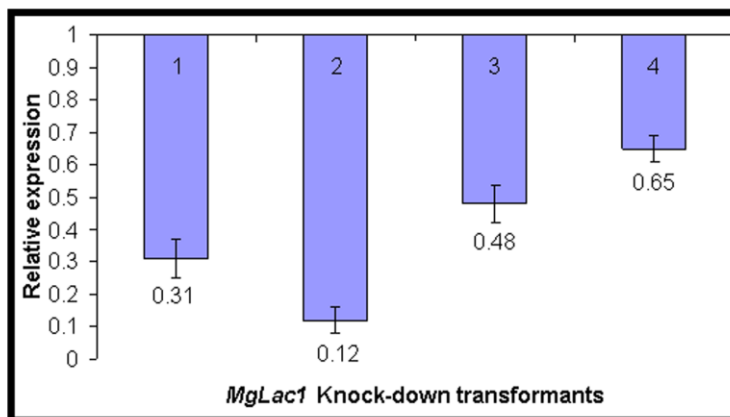
B.

Figure 28: Relative expression of *Mglac*1 *and MgLac*2 gene in knock-down transformants.

(A) *MgLac*1 knock-down transformants: The relative expression level was compared with wild type B157.

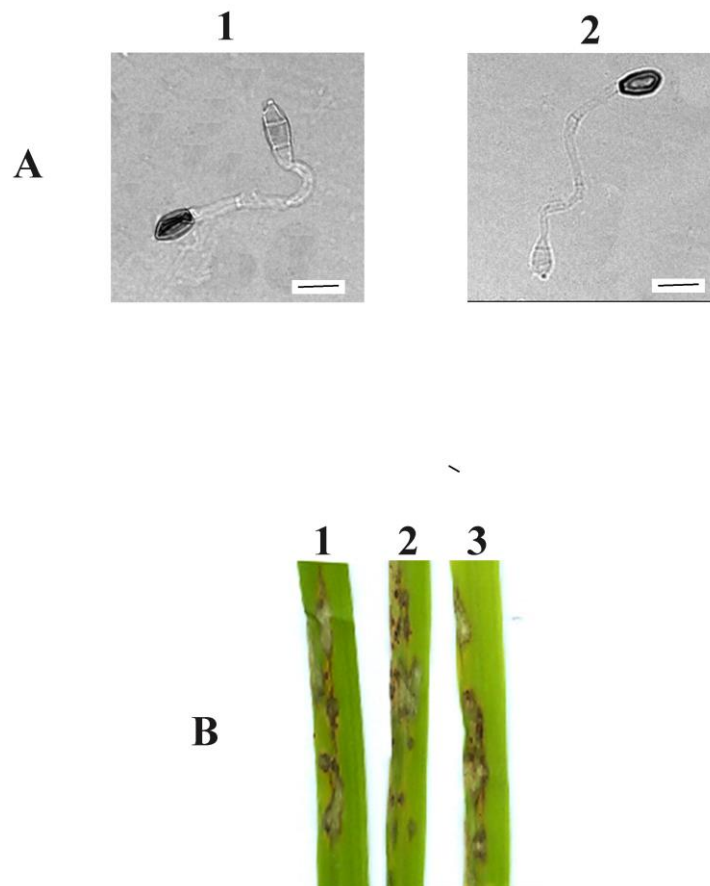The values given are the average of triplicates. Bars indicate mean ± SD.

(B) *MgLac*2 knock-down transformants: The relative expression level was compared with wild type B157.

The values given are the average of triplicates. Bars indicate mean ± SD.

Figure 29: Representative appressorium formation and infection assay of *MgLac*1 knock-down transformants.

(A) *MgLac*1.2 (88%) knock-down transformants are able to form appressoria on gel bond film. Conidia were allowed to germinate on hydrophobic side of gel bond film for 16 h and visualised under microscope. 1, B157; 2, *MgLac*1 knock-down transformant. Bar represents 20μM

(B) Barley infection - Spray inoculation infection assays were performed with spore suspension (~10^5 spores/ml) and disease symptoms were recorded after 5 days. 1- B157; 2, 3- *MgLac*1.2 (88%) knock-down transformant.
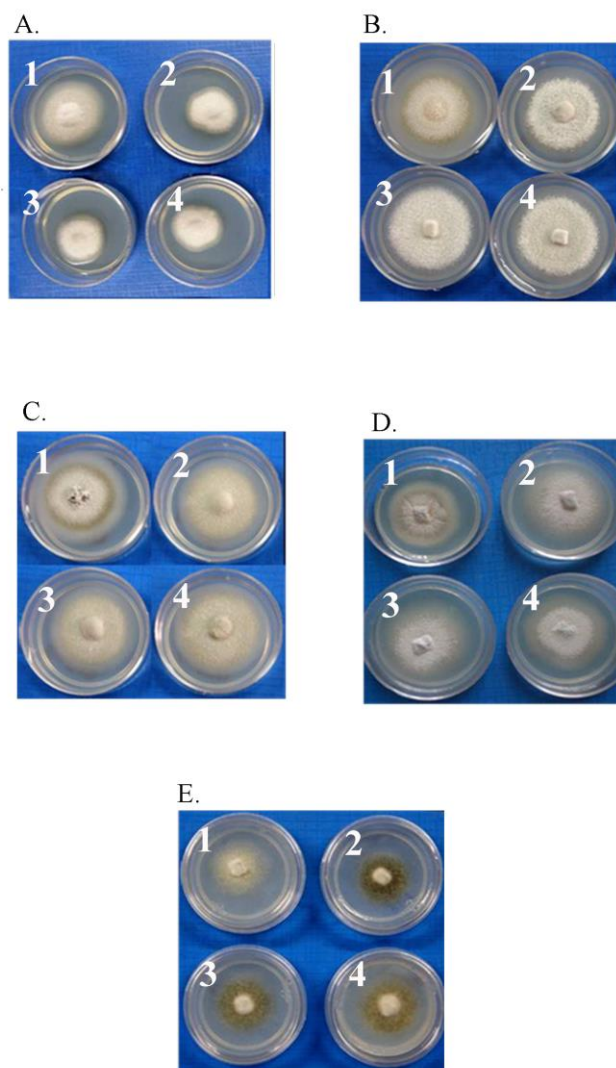
Figure 30: Effect of different metals on growth of *MgLac*1 knock-down transformants. Growth of wild type B157 and *MgLac*1 knock-down transformants (KT) on YEG agar media supplemented with **(A)** EDTA, 200µM; **(B)** Iron, 200µM; **(C)** Copper, 200µM; **(D)** NaCl, 1M; **(E)** CaCl$_2$, 200mM. Medium plates were inoculated with 5 mm^2 mycelial plug and grown at 28^{0}C for 7 days.

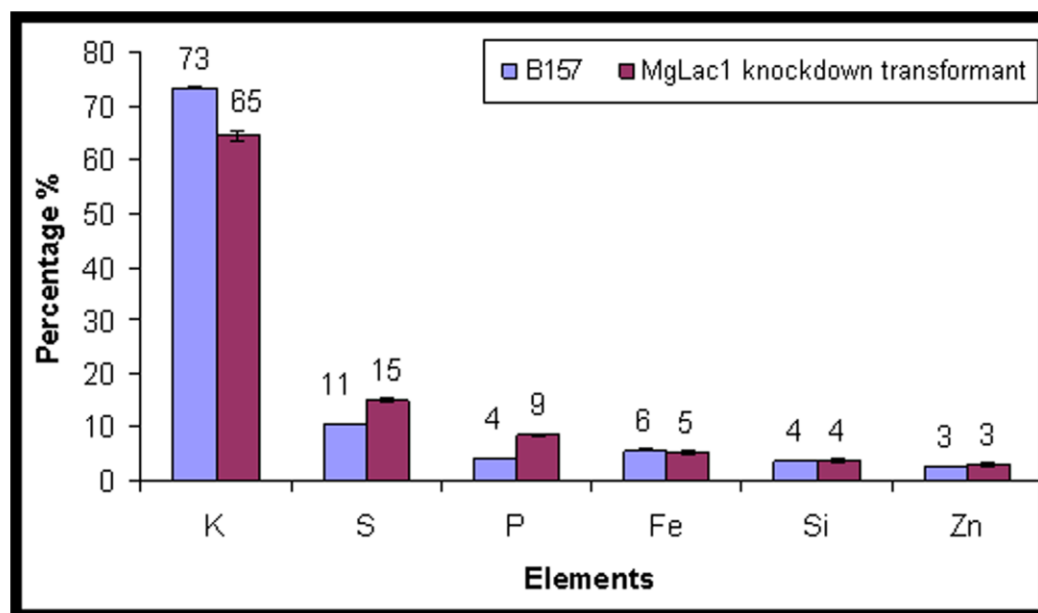(1, B157; 2, *MgLac*1.1; 3, *MgLac*1.2 and 4, *MgLac*1.3)

Figure 31: Elemental analysis of *MgLac*1 knock-down transformants.

X – Ray fluorescence spectroscopy was used for elemental analysis of wild type B157 and *MgLac*1.2 (88%) knock-down transformants. The values plotted are average of duplicates.
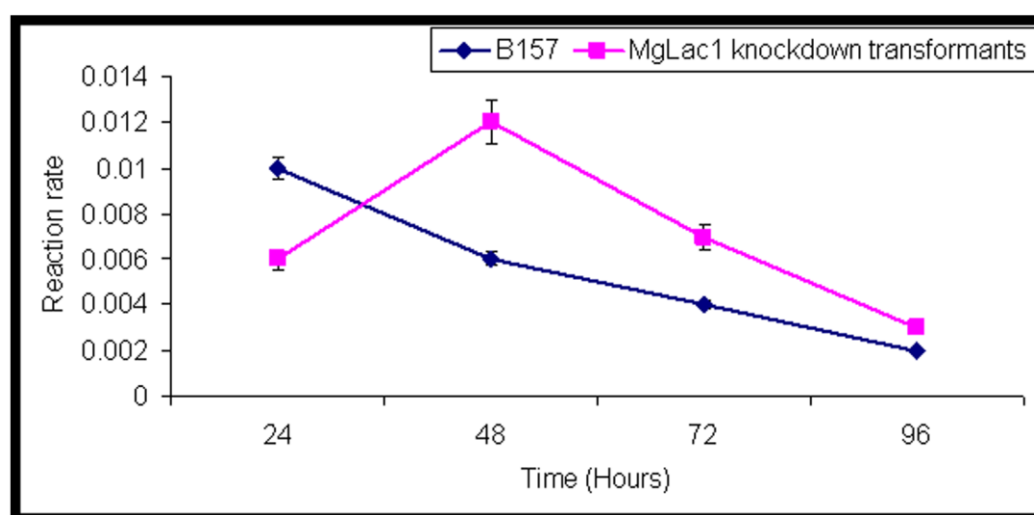
.

Figure 32: Profile of laccase activity in wild type B157 and *MgLac*1.2 (88%) knock-down transformant.

Laccase activity was estimated in wild type B157 and *MgLac*1.2 (88%) transformant at 24h, 48h, 72h, and 96h.

The values plotted are average of triplicates. Bars indicate mean

± SD

autolysis of mycelia after incubation on oatmeal agar plate for 7- 8 days **(Figure 33.B)**. Autolysis began at the centre of the mycelium and radiated outward.

Further cell wall integrity was tested by treating an equal amount of mycelia from wild type strain and knock-down transformants with cell-wall-degrading enzyme. The knock-down transformants were hypersensitive to the lytic enzyme treatment, and produced protoplasts at a rate faster than wild type fungus, i.e. 5.53×10^6 protoplasts were produced after 90 min of lytic enzyme treatment in the knock-down transformants in comparision to 2.57×10^6 protoplasts in the wild type in the same time, suggesting that knock-down transformants were compromised for their cell wall integrity **(Figure 34).**

3.20 Infection assays of *MgLac* 2 knock-down transformants

The ability of the knock-down transformants to cause infection was investigated using barley explant/ spray inoculation infection assays. The *MgLac*2.1 knock-down transformant consistently failed to cause infection on barley leaves **(Figure 35.A)**. Further, the invasive growth of knock-down transformants was examined by abrading the leaves with a needle before inoculating the spore suspension. This allowed direct entry of the fungus into host tissues through a wound site without appressorium. The wild type strain as well as *MgLac*2.1 knock-down transformant developed disease lesions **(Figure 35.B)**. The functionality of knock-down transformants appressoria, penetration and invasive growth were monitored using onion epidermis. Wild type appressoria penetrated into epidermis cells and developed ramifying invasive hyphae, whereas appressoria from the *MgLac*2.1 transformant failed to penetrate the onion epidermis **(Figure 35.C)**.
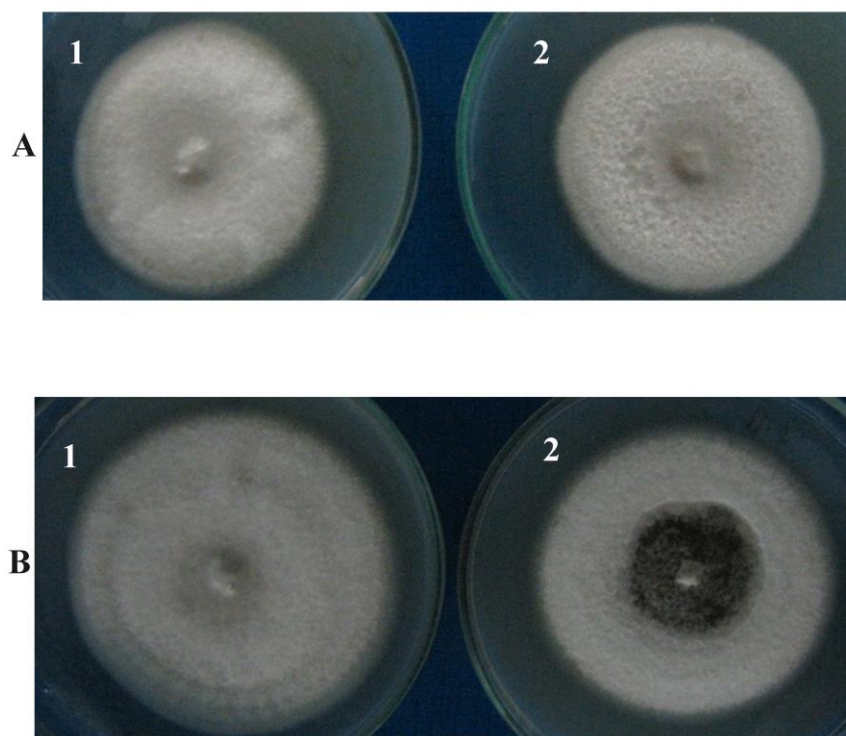
Figure 33: Representative morphology of *MgLac*2 knock-down transformants.

(A) *MgLac*2 knock-down transformants were having less aerial hyphae than the wild type B157. Transformants were allowed to grow on oatmeal agar plate for 5 days. 1, B157; 2, *MgLac*2.1 (88%) knock-down transformant.

(B) Autolysis phenotype of *MgLac*2 knock-down transformants on oatmeal agar plates. Transformants were allowed to grow on oatmeal agar plate for 8 days. 1, B157; 2, *MgLac*2.1 (88%) knock-down transformant.
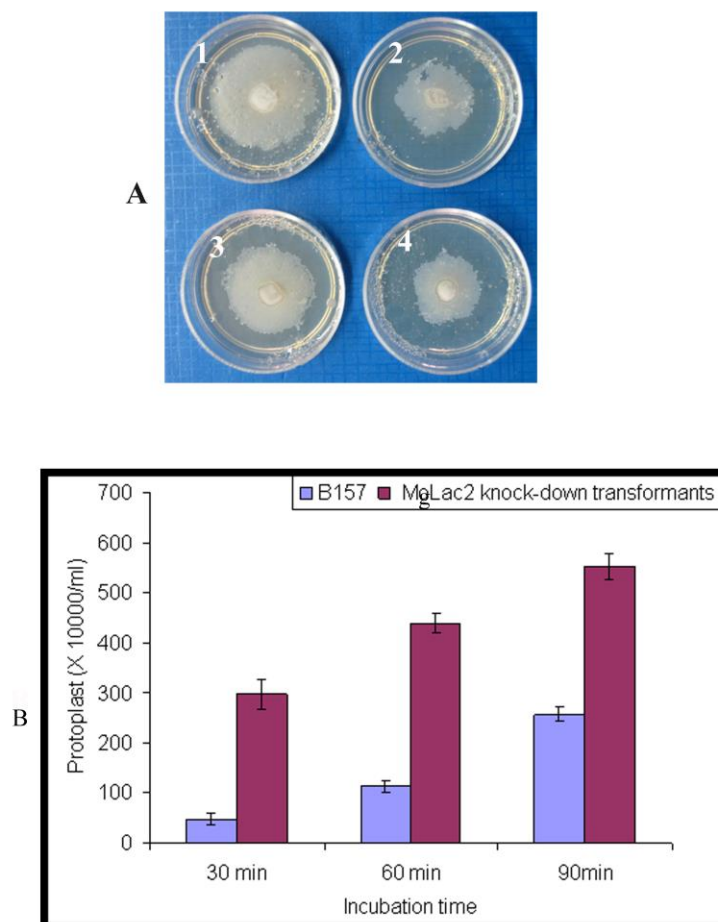
Figure 34: Treatment of *MgLac*2 knock-down transformants with cell-wall-degrading enzymes.

(A) Growth of wild type B157 and *MgLac*2 knock-down transformants on YEG agar media supplemented with lysing enzyme (2mg/ml). Medium plates were inoculated with 5 mm^2 mycelial plug and grown at 28^{0}C for 7 days. 1- B157; 2, *MgLac*2.1; 3, *MgLac*2.2 4, *MgLac*2.3 - knock-down transformants.

(B) Protoplast production by cell wall degrading enzyme. The protoplast production was quantified in using counted using a hemacytometer at regular time intervals in triplicates. Protoplast production of *MgLac*2.1 (88%) knockdown transformant was compared with wild type B157.
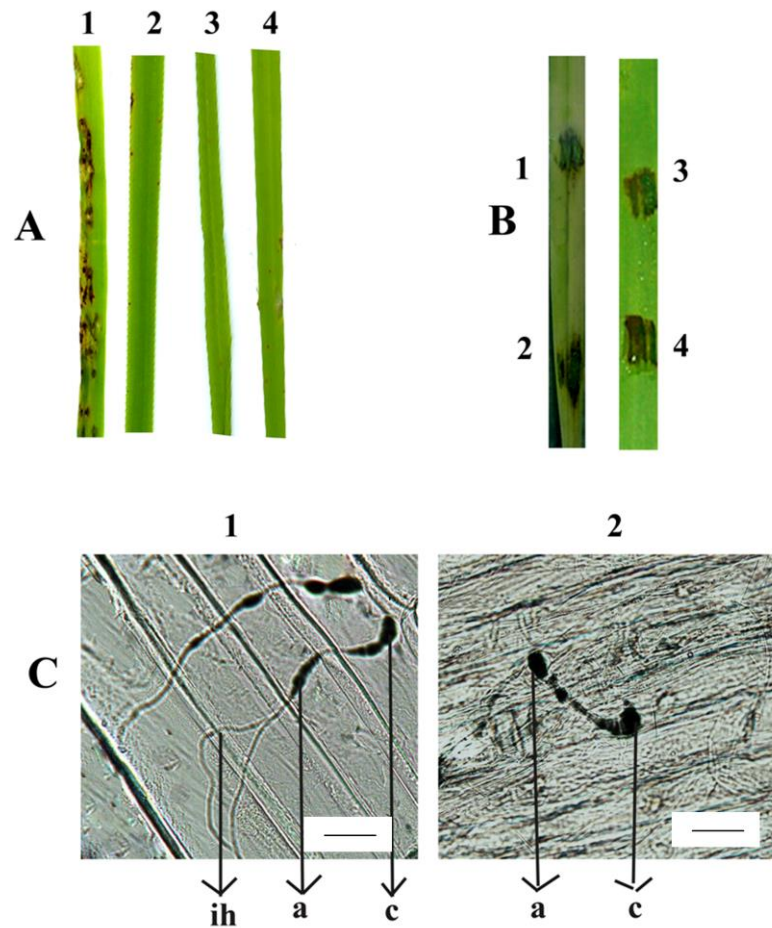
Figure 35: Representative infection and penetration assay of *MgLac*2 knock-down transformants.

(A) Barley infection - Spray inoculation infection assays were performed with spore suspension (~10^5spores/ml) and disease symptoms were recorded after 5 days. 1- B157; 2,3,4 - *MgLac*2.1 (88%) knock-down transformant.

(B) Barley infection after wounding - Leaves were abraded with a needle before inoculation. 1, B157; 2,3,4, *MgLac*2.1 knock-down transformants.

(C) *MgLac*2.1(88%) knock-down mutant unable to penetrate onion epidermis. Conidia were allowed to germinate onion epidermis for 48h and visualised under microscope after fixing the fungus with lactophenol. A, appresorium; S, spore; IH, infectious hyphae. Bar represents 20μM

3.21 *MgLac* 2 knock-down transformants are sensitive to metals

Metal restricted sensitivity assays were carried out in the presence EDTA (200μM) *MgLac2* knock-down transformants showed less growth in the presence of EDTA. The transformants showed growth upto ~62 % of the wild type **(Figure 36.A).** In presence of 200 μM iron **(Figure 36.B)** and copper **(Figure 36.C)** the growth of the transformants was significantly affected. The transformants showed ~65% and ~74% growth reduction when compared to wild type in presence of iron and copper, respectively.

Knock-down transformants became more sensitive to antifungal drug miconazole **(Figure 36.D)**. The growth of transformants was 20% less than the wild type. Further knock-down transformants were tested for sensitivity to agents that challenge cell wall integrity and reduced growth was observed on medium containing SDS **(Figure 36.E)**. It showed 25% less growth than the wild type.

As the knock-down transformants showed sensitivity towards different metals, elemental analysis of wild type *M. grisea* and knock-down transformants was done using X-Ray fluorescence spectroscopy. Considerable differences were observed in the iron and zinc content of the transformants. The internal iron and zinc content of the transformants were ~ 68% and ~ 55%, respectively, compared to the wild type (**Figure 37**).

3.22 Lipid mobilisation

During appressorial development, lipid reserves in conidia are rapidly transferred to appressoria where they are degraded and supplied as the source of glycerol. To determine whether the lipid mobilization in *MgLac2* knock-down transformants was affected, lipid

bodies were monitored during appressorial morphogenesis via Nile red staining. In wild type *M. grisea* the translocation of the lipid droplets from conidia to appressoria took place within 12h followed by lipid degradation in conidia during appressorium maturation (24h). However, *MgLac2* knock-down transformants showed slow translocation of the lipid droplets from conidia to appressoria (24h) and followed by even slower degradation in conidia (48h) (**Figure 38**).

3.23 Profile of laccase activity in B157 and *MgLac2* knock-down transformants

Wild type B157 and the *MgLac*2.1(88%) knock-down transformants were grown in liquid culture and the laccase activity was checked at different time points. After 24 hrs the laccase activity in *MgLac*2 knock-down transformants was slightly less than the wild type and almost the same after 48 hrs (**Figure 39**).

3.24 Expression of other multicopper oxidases in the knock-down transformants

The targeted deletion of *MGG_00551.5* and *MGG_02876.5* did not affect the growth rate, conidiation and pathogenicity as compared to wild type strain (Chen *et al.*, 2009) Interestingly, antisense of *MGG_02876.5* led to pathogenicity impairment in *M. grisea*. Therefore the transcripts levels other multicopper oxidases were also checked in *MgLac1* (**Figure 40**) and *MgLac2* (**Figure 41**) knock-down transformants to look for some trend in relative expression of other multicopper oxidases in knockdown transformants. Variations in the transcript level of other multicopper oxidases were observed.

3.25 eGFP silencing with siRNA

Optimisation of siRNA silencing was done using eGFP expressing *M. grisea.* siRNA for

eGFP were generated as mentioned in the materials and methods. Briefly, two separate

PCR reations were carried out for sense and antisense fragments with the specific primers

(Figure 42.A) and *in vitro* transcription reactions were carried out for both sense and

antisense fragments. The two transcription reactions were mixed **(Figure 42.B)** and

siRNA generated using shortcut RNase (18-23 bp) were checked on 12 % PAGE **(Figure**

42.C).

Protoplast transformation of *M. grisea* was carried out with the eGFP siRNAs (100 nM).

eGFP fluorescence was observed at regular time intervals after transformation. Silencing

of eGFP fluorescence was highest after 24 hours of transformation and was observed till

72 hrs. No difference in GFP fluorescence was observed after 96 hrs **(Figure 43)**.

3.26 Silencing five multicopper oxidases with siRNAs

Five multicopper oxidases were always silenced in *MgLac2* knock-down transformants

ie, *MGG_02876.5, MGG_00551.5*, *MGG_07771.5, MGG_11608.5* and *MGG_05790.5*.

Silencing of these 5 multicopper oxidases with the specific siRNAs generated was carried

out. After transformation the selection was done on media containing Sodium Dodecyl

Sulphate (0.025%). 60-75% reduction in the number of colonies with *MGG_07771.5*

siRNA was observed **(Figure 44)**. No such reduction was observed with other

multicopper oxidase siRNAs.

3.27 *MGG_07771.5* has a transmembrane domain

Wolf PSORT predicted *MGG_07771.5* protein to have plasma membrane localisation. HMMTOP predicted the presence of transmembrane domain from 48 to 72 amino acid residues. 47 amino acids at the N-terminal of the protein are predicted to have cytoplasm localisation. Rest of the protein towards the C-terminal is predicted to have extracellular localisation **(Figure 45)**. None of the other *M. grisea* predicted laccases showed transmembrane localization.

---/---
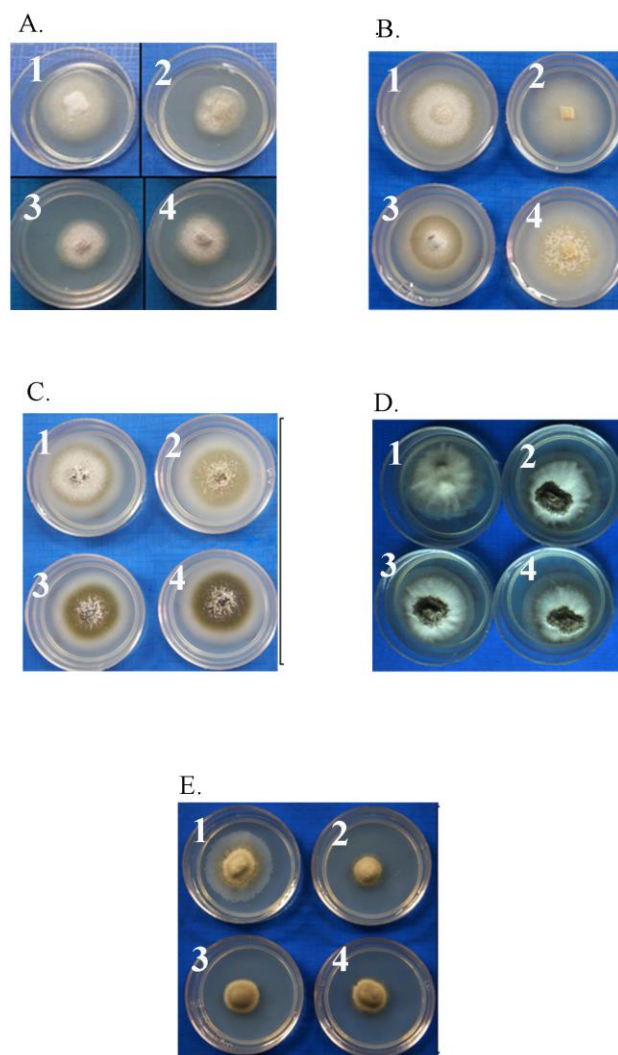
Figure 36: Effect of different metals and chemicals on growth of *MgLac*2 knock-down transformants. Growth of wild type B157 and *MgLac*2 knock-down transformants (KT) on YEG agar media supplemented with **(A)** EDTA, 200µM; **(B)** Iron, 200µM; **(C)** Copper, 200µM; **(D)** Miconazole, 2µg/mL; **(E)** SDS, 0.025%. Medium plates were inoculated with 5 mm^2 mycelial plug and grown at 28^{0}C for 7 days.
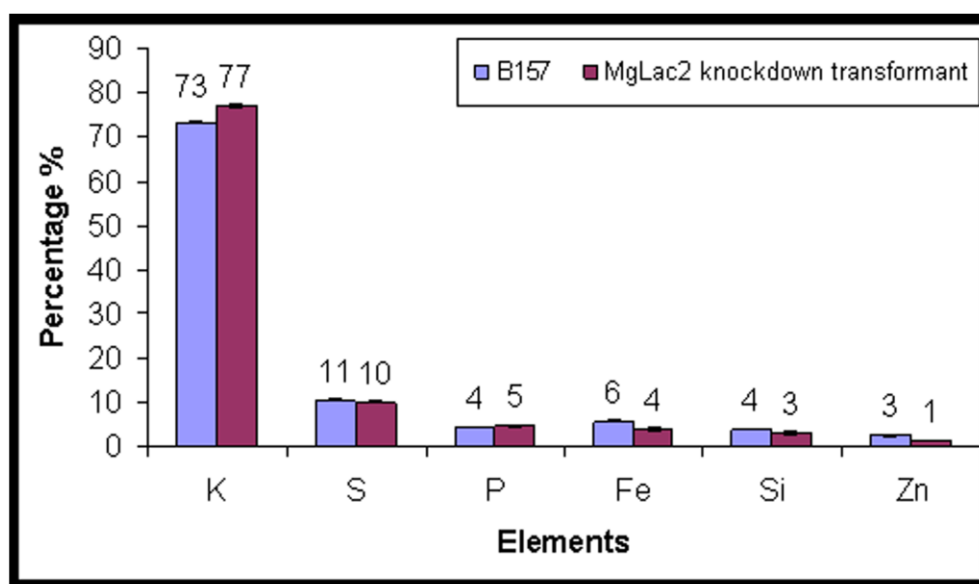
(1, B157; 2, *MgLac*2.1; 3, *MgLac*2.2 and 4, *MgLac*2.3)

Figure 37: Elemental analysis of *MgLac*2 knock-down transformants.

X – Ray fluorescence spectroscopy was used for elemental analysis of wild type B157 and *MgLac*2.1 (88%) knock-down transformant. The values plotted are average of duplicates.
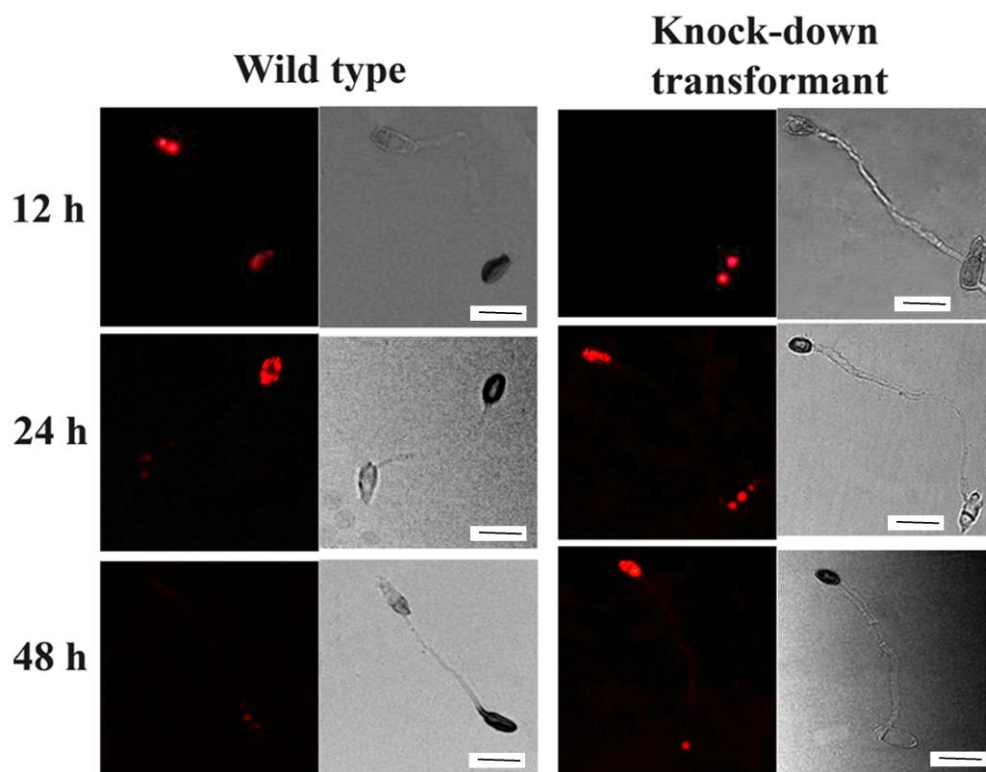
Figure 38: Cellular distribution of lipids in wild type strain B157 and *MgLac*2.1 (88%) knock-down transformants. Conidia from wild type B157 and knock-down transformants were allowed to form appressoria on hydrophobic side of gel bond film. The films were removed at different time intervals and stained with Nile red. For each time point, bright field (right panel) and corresponding epiflourescence (left panel) images are presented. **B157** - Lipid droplets translocated into appressoria (12h), lipid degradation occurred rapidly during appressorium maturation (24h), and fully melanised appressoria were almost entirely devoid of lipid droplets (48h). *MgLac*2.1 **knock-down transformants** - Lipid droplets showed slow translocation of the lipid droplets from conidia to appressoria (24h) and followed by even slower degradation in conidia (48h). Bar represents 20µM
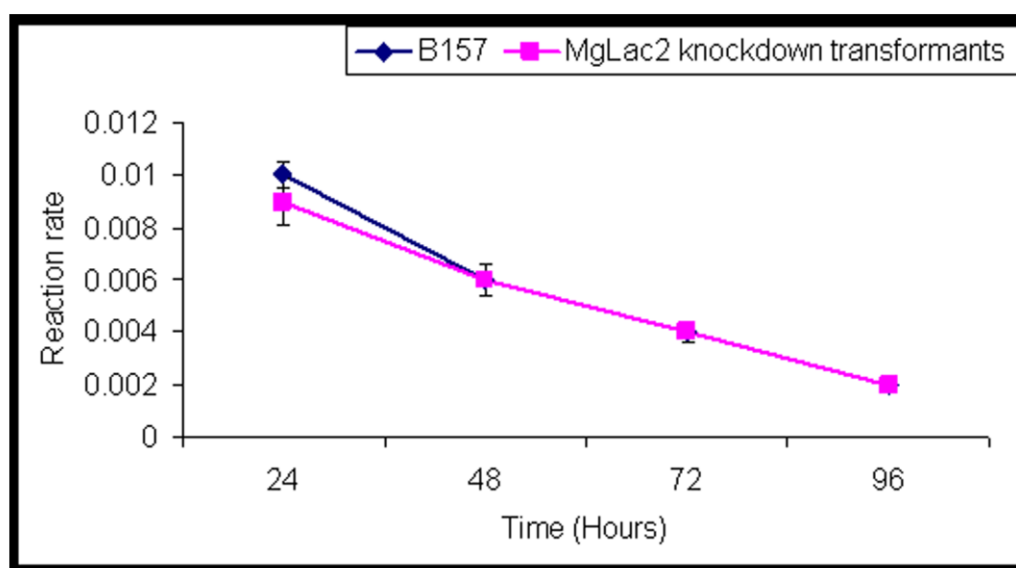
Figure 39: Profile of laccase activity in B157 and *MgLac*2.1(88%) knock-down transformants.

Laccase activity was estimated in B157 and *MgLac*2.1(88%) transformant at 24h, 48h, 72h, and 96h. The

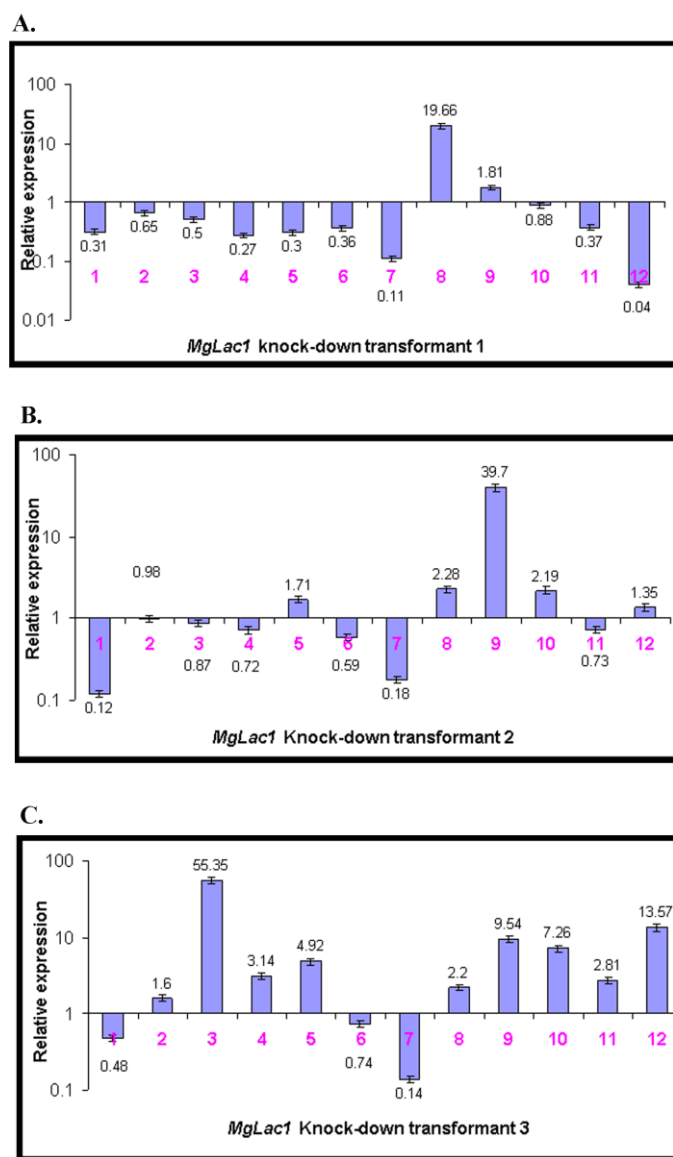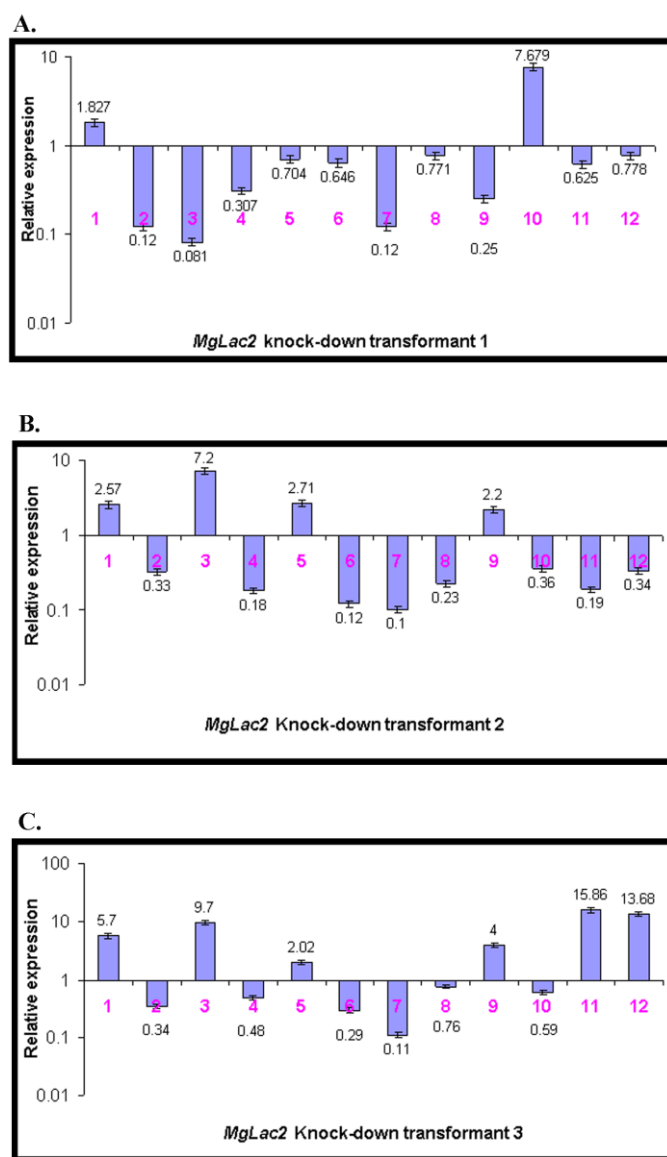values plotted are average of triplicates. Bars indicate mean ± SD.

Figure 40: Relative expression of other multicopper oxidases in *MgLac*1 knock-down transformants. (1, MGG_08127; 2, MGG_02876; 3, MGG_13464; 4, MGG_05790; 5, MGG_09139; 6, MGG_11608; 7, MGG_00551; 8, MGG_07771; 9, MGG_07220; 10, MGG_02156; 11, MGG_14307 and 12, MGG_09102). The relative expression level was compared with wild type B157. The values given are the average of triplicates. Bars indicate mean ± SD.

(A) *MgLac*1.1 knock-down transformant, **(B)** *MgLac*1.2 knock-down transformant and *(***C)** *MgLac*1.3 knock-down transformant

Figure 41: Relative expression of other multicopper oxidases in *MgLac*2 knock-down transformants. (1, MGG_08127; 2, MGG_02876; 3, MGG_13464; 4, MGG_05790; 5, MGG_09139; 6, MGG_11608; 7, MGG_00551; 8, MGG_07771; 9, MGG_07220; 10, MGG_02156; 11, MGG_14307 and 12, MGG_09102). The relative expression level was compared with wild type B157. The values given are the average of triplicates. Bars indicate mean ± SD.

(A) *MgLac*2.1 knock-down transformant, **(B)** *MgLac*2.2 knock-down transformant and **(C)** *MgLac*2.3 knock-down transformant
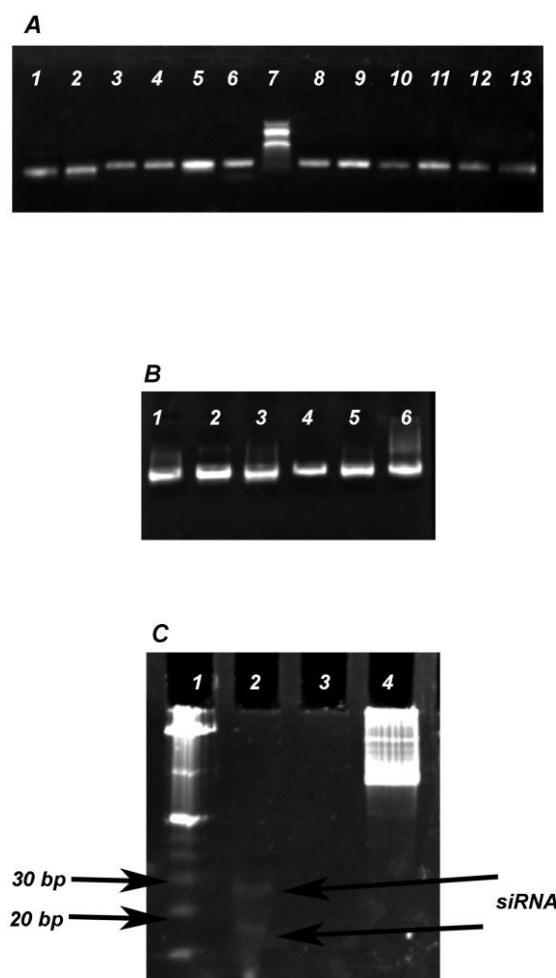
Figure 42: Preparation of dsRNA and siRNA of 5 multicopper oxidases.

(A) Two separate PCRs were carried out for sense and antisense fragments of all the 5 multicopper oxidases (MGG_02876.5, MGG_00551.5, MGG_07771.5, MGG_11608.5 and MGG_05790.5) and GFP with the primers designed.

(B) *in vitro* transcription reactions were carried out for both sense and antisense fragments separately and then the sense and antisense fragments of each multicopper oxidase and GFP were mixed for siRNA preparation.

(C) Representative picture of siRNA prepared (18-23 bp), which were checked on 12 % PAGE. Lane1: ladder, Lane2: siRNA, Lane3: nil and Lane4: mix of sense and antisense fragments
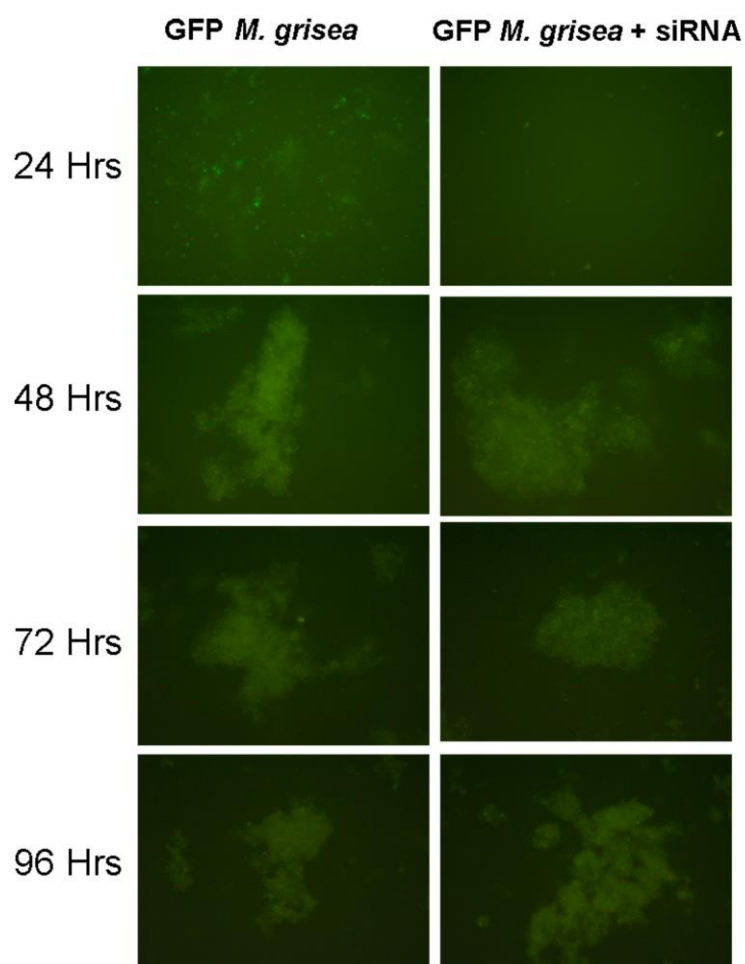
GFP *M. grisea*   **GFP *M. grisea* + siRNA**

24 Hrs

48 Hrs

72 Hrs

96 Hrs

Figure 43: Reduction in the GFP fluorescence was observed under microscope after 24, 48, 72 and 96 hours of transformation with siRNA of GFP. Maximum silencing of GFP was observed after 24 hrs of transformation. Silencing was observed tills 72 hrs. From 96 hrs no difference in GFP fluorescence was observed between transformed and untransformed *M. grisea.*
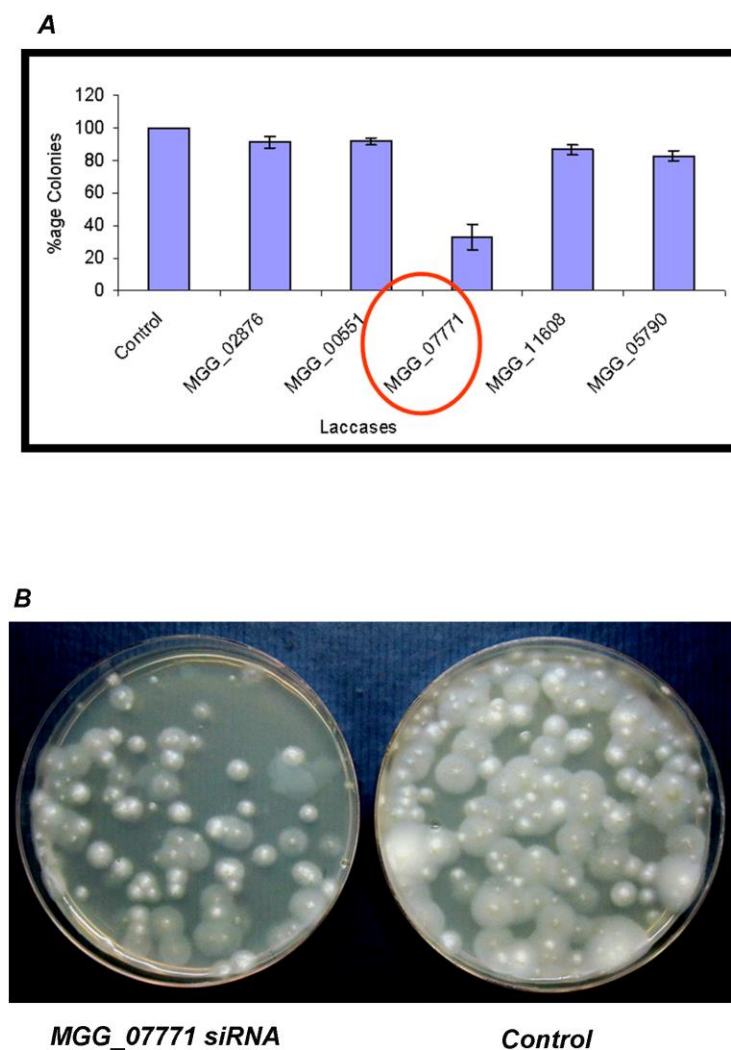
Figure 44: siRNA based protoplast transformation of *M. grisea.*

(A) Transformants of 5 multicopper oxidases were selected and the number of colonies counted. 60-75% reduction in the number of colonies with *MGG_07771.5* siRNA was observed. The values given are the average of triplicates. Bars indicate mean ± SD.

(B) Representative picture of the number of colonies on the selection plate, control versus *MGG_07771.5* siRNA
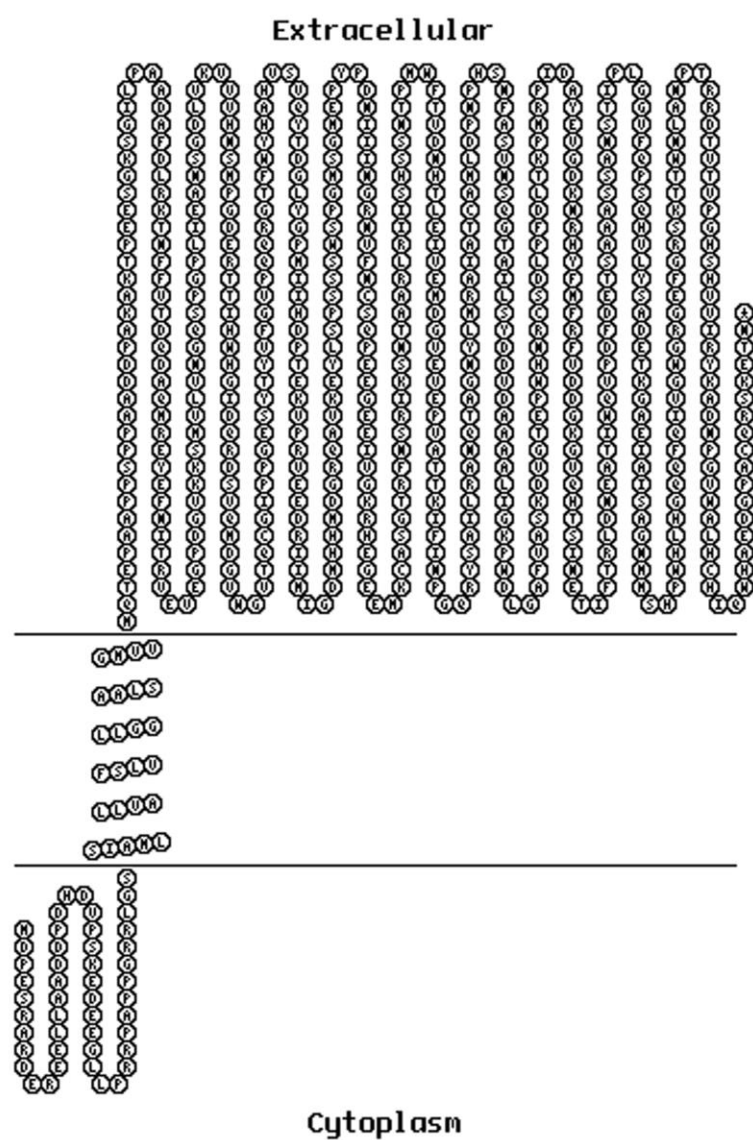
Figure 45: Transmembrane localisation prediction of MGG_07771. Basic TOPO2 output image of the prediction (HMMTOP prediction).